I – Introduction

All cells are variations on a basic structural theme: a package of highly structured cytoplasm contained within a lipid barrier. The cytoplasm is subdivided by internal membrane system into several compartments specialized for particular function. The mechanical strength and capacity to change shape of a cell, its own movement and internal action are largely provided by an intracellular network of specialized polymers, the cytoskeleton. The actin cytoskeleton involves a multitude of proteins and regulatory mechanisms implicated in assembly, disassembly and organization of actin filaments, making this system vulnerable to genetic alterations that may cause diseases, such as cancer. In cancer cells, structural and functional perturbations of the actin cytoskeleton correlate with higher proliferation rates and uncontrolled movement (Giganti and Friederish, 2003). Therefore, the study of the actin dynamics during tissue morphogenesis is important for cancer therapeutics.

1 – Drosophila *as a model system*

Drosophila melanogaster is one of the most used model organisms and is commonly known as the "fruit fly". Among many advantages of using flies as a research model are their short life cycle, high fecundity, small genome, easy and low cost culturing and their powerful genetic tools (reviewed in St. Johnston, 2002). Furthermore, 197 out of 287 human genes, known to cause disease when misregulated have *Drosophila* homologues that can produce very similar symptoms when misregulated in flies (reviewed in St. Johnston, 2002).

1.1 – Advantage of using *Drosophila* genetics

Genetic tools commonly used in *Drosophila* allow the identification and characterization of genes that are involved in a wide range of biological processes

(reviewed in St. Johnston, 2002). Some of such genetic tools available are the balancers chromosomes, the phenotypic markers and non-recombination in males. The balancer chromosomes are chromosomes with one or more inverted segments that suppress recombination and allow lethal mutations or transgenes to be maintained without selection. A large number of phenotypic markers, both recessive and dominant, are available and allow the selection of flies carrying the chromosome of interest, by eye, body, bristle, larval and wing phenotype. By using Mendel's law and following a dominant phenotypic marker, it's easy to successfully follow a multi-generation cross. Also, there is another powerful technique available which is the P-elements transformation. Using this technique it is possible to introduce any gene of interest within the *Drosophila* genome as soon as the construct of interest has been placed between P-elements. The P-elements are transposable pieces of DNA that randomly insert into genomic DNA with the help of the transposase enzyme. Transgenic flies are selected using a variety of phenotypic markers such as eye color, body color or resistance to antibiotics (Socolish, 2003).

Moreover, there is another useful genetic tool used to analyze gene function known as genetic mosaics that will be frequently used throughout this work. By genetic mosaic technique, genetic changes can be induced in a subset of cells or tissues in an individual organism and examine genetic changes that would be otherwise lethal if applied to the entire organism (see Materials and Methods) (Blair, 2003).

1.2 – The *Drosophila* life cycle

The developmental period of *Drosophila* depends at which temperature the flies are grown. Drosophila undergoes a process of metamorphosis which proceeds as follows: embryo, larvae, pupae and ends in the adult fly. The shortest developmental time (egg to adult) takes 7 days and it is achieved at 28ºC. The developmental time increase at higher temperatures due to heat stress. Under ideal conditions, the development time at 25°C is 8.5 days, as it is shown in Fig. 1.1. At room temperature the whole cycle takes 12 days. Females lay some 400 eggs (embryos) per day into their food (Ashburner *et al*., 2005).

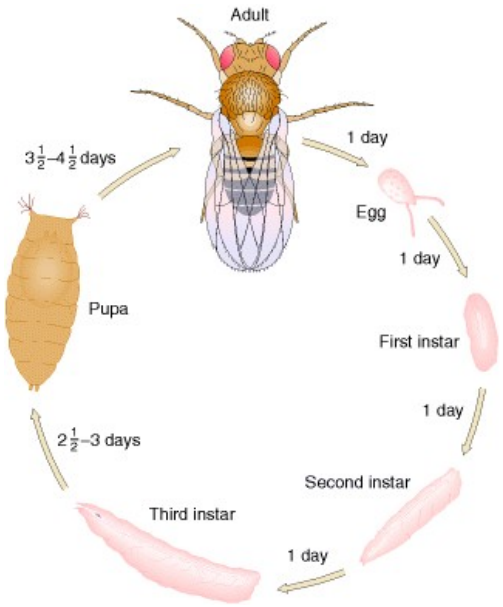

Figure 1.1 – Schematic representation of *Drosophila melanogaster* life cycle at 25ºC (adapted from Griffiths *et al*., 2000).

1.3 – *Drosophila* imaginal discs are typical epithelial structures

1.3.1 – Epithelial structure of the wing imaginal disc

Each *Drosophila* external adult structure (such as wings, leg, eyes and antennas) derive from internal structures called imaginal discs (as shown in Fig.1.5). Imaginal discs form during embryogenesis from small clusters of cells (about 40 cells for the wing disc). That proliferate during the whole larval development to form folded, single layer, epithelial sacs (about 10000-50000 cells for the wing disc) (reviewed in St. Jonhston, 2002).

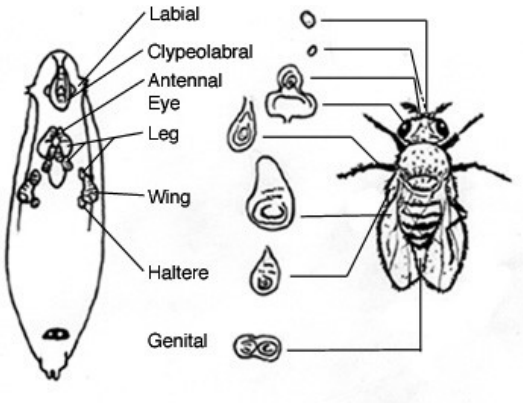

Figure 1.5 – Location and identification of *Drosophila* imaginal discs (adapted from Carballo and Hwang, 2000).

Each of these sacs consists of a columnar epithelium covered by a peripodial membrane (Fig. 1.7) (Schock and Perrimon, 2002). The columnar cells are a laterally coherent sheet polarized along the apico-basal axis. These epithelial cells contain adherens junctions (AJ) composed mainly of E-cadherin and α- and β-catenin (in *Drosophila* encoded by *armadillo*). The AJ localize apically and links the actin cytoskeleton (also polarized) of neighboring cells (Fig.1.6). Apical to the AJs, *Drosophila* has two complexes that are involved in regulating the establishment and maintenance of epithelial polarity. These complexes are the Baz/Par-6/aPKC complex and Crb/Stardust/Patj complex (Fig.1.6). Present basal to AJ, exists the septate junctions that are formed by Dlg/Scribble/Lgl complex (Gibson and Perrimon, 2003) (Fig.1.6).

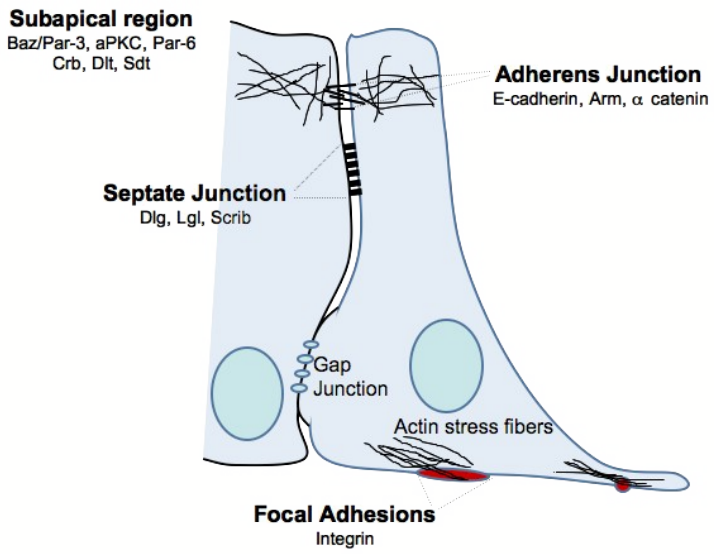

Figure 1.6 – Schematic representation of a *Drosophila* epithelial cell (modified from Schock and Perrimon, 2002). The major junctional complexes are represented: the apically localized subapical region, the adherens junction and the septate junction.

Many tissues are composed of epithelial sheets that function as a protection from the external environment and separate two different chemical milieus (Schock and Perrimon, 2002). Imaginal discs are therefore considered an interesting model to study epithelial morphogenesis, because they are true epithelial tissue, which are differentiated and easy to dissect, since they are floating in the larvae. In addition, their advantages rely mostly on the great success of *Drosophila* as a genetic model organism (referred in Section 1).

1.3.2 – Patterning of the wing imaginal disc

Growth and patterning of wing imaginal discs occurs during larval development. The late third instar disc is extensively patterned by complex expression patterns of genes, dividing the disc into territories called "compartments" (Whittle, 1990). The first compartment established is the anterior-posterior (A/P) boundary during embryonic stage (Cohen, 1993). This boundary requires the *engrailed* gene product in the posterior compartment for its maintenance (Lawrence and Morata, 1976). The other boundary that

occurs during wing development is the dorsal-ventral (D/V) boundary and it is formed during the second larval instar. This happens by the relationship between the epidermal growth factor (EGF) and Wingless (Wg) signaling (Klein, 2001). The two boundaries observed in the wing imaginal disc are represented in Fig. 1.7. Along these axis we can observe 3 main morphological regions: the wing blade, hinge and notum. The blade (green), which will give rise to the adult wing, the hinge (yellow) that will give rise to the structures that attaches the wing to the thorax of the fly and finally the notum that will give rise to the thorax of the adult fly (Butler *et al*., 2003).

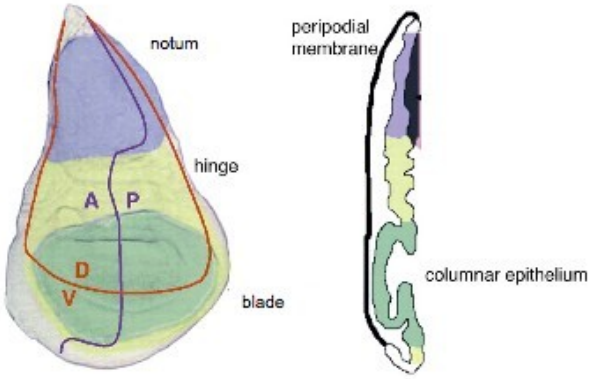

Figure 1.7 – Structure of the wing imaginal disc (adapted from Butler *et al*., 2003). Third instar wing imaginal disc showing the anterior-posterior and dorsal-ventral compartments boundaries and major regions in the disc. Blue indicates the notum, yellow indicates the hinge and green indicates the blade.

Another system subdivides the disc along the proximal-distal axis early in development. In the proximal-distal patterning, the wing disc forms both distal (wing) and proximal (notum) structures. It is known that *Decapentaplegic* (*dpp*) gene is required for proximal-distal patterning of all adult appendages (Posakony *et al*., 1990), while *apterous* (*ap*), *scalloped* (*sd*), *vestigial* (*vg*) and *wingless* (*wg*) genes are specifically required for formation of the wing region of the disc (Lindsley and Zimm, 1992). This last four genes can be subdivided in two classes that reflect either an early or late requirement in disc development. Therefore, *vg* and *sd* are required later in development (during the third larval instar). In contrast, *ap* is required before wing specification to established the proper domains of *sd* and *vg* expression. Interestingly, *wg* has the earliest requirement and influences both the notum/wing and dorsal/ventral boundaries. *wg* plays a key role in positioning *ap* expression and promoting *vg* expression, suggesting that *wg*

is on the top of genetic regulatory hierarchy guiding wing formation (Williams et al, 1993). Wg was one of the first members of Wnt family to be identified (Baker, 1987), and its function is required throughout development in a wide range of patterning events at different times and in different tissues (Cadigan and Nusse, 1996). In the case of the wing imaginal disc, Wg is involved in the specification of the wing margin, which is required for the promotion of cell proliferation and patterning of wing cells (Neumann and Cohen, 1997). Wg is expressed in the two concentric rings of the hinge (Neumann and Cohen, 1996). Thus, this secreted signaling molecule is a developmental regulator of epithelial tissue growth in flies.

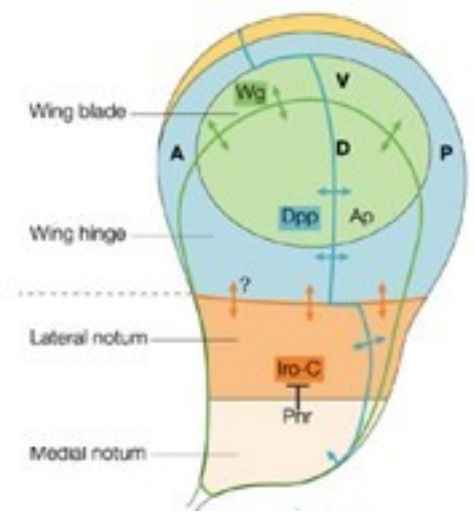

Figure 1.8 – Schematic representation of a wing imaginal disc showing the major patterning genes involved in the proximo-distal axis and the different regions of the disc (adapted from Gómez-Skarmeta *et al*, 2003).

1.3.3 – Growth control of the wing imaginal disc

The development of a functional organ requires not only patterning mechanisms that confer proper identities for its constituent cells, but also growth-regulatory mechanisms that specify the final size of the organ (Barolo and Posakony 2002). In *Drosophila*, the same extracellular signaling pathways responsible for pattern formation also directly regulate cell proliferation. This naturally links growth and patterning during development (Baker, 2007). There are several developmental regulators of epithelial

tissue growth in flies, the already mencioned EGF, Wg and Decapentaplegic (DPP), and also Notch. These growth regulators interact with pathways and control networks, such as the Hippo signal transduction pathway, which is required to restrict cell and tissue growth in *Drosophila*. The Hippo signaling pathway is important during the development and it is a vulnerable target for misregulation in cancer. The Hippo pathway consists of several negative growth regulators acting in a kinase cascade that ultimately phosphorylates and inactivates Yorkie (Yki), a transcriptional co-activator that positively regulates cell growth, survival, and proliferation. The upstream components Fat, Merlin and Expanded transduce extracellular signals that promote the phosphorilation and activation of Warts by Hippo. In turn, Salvador and Mats activate the kinase activity of Hippo and Warts, respectively. Activated Warts phosphorilates and inactivates the transcriptional co-activator Yorkie, promoting tissue growth (reviewed in Saucedo and Edgar, 2007).

Recent studies have shown that inactivation of Hippo signaling allows cells in the developing fly epithelium to outcompete between them (reviewed in Saucedo and Edgar, 2007). This mechanism, called cell competition, compares cells within a growing population and eliminates the weaker ones by JNK-mediated apoptosis (Moreno *et al.*, 2002). The winner cells not only survive but also proliferate to fill the space left by the disappearing cells. One required property of cell competition is that the loser cells can survive if they are surrounded by cells of the same genotype. So, the elimination of a cell by this mechanism is a non-autonomous process and is caused by the presence of wild-type cells (Moreno *et al*., 2002).

2 – The actin cytoskeleton

Tissue patterning must be translated into morphogenesis through cell shape changes mediated by remodeling of the actin cytoskeleton (Janody and Treisman, 2006). The actin cytoskeleton plays an important role in numerous cellular processes in all eukaryotic organisms. It is responsible for the generation and maintenance of cell morphology and polarity, in endocytosis and intracellular trafficking, in contractility, motility and cell division. Actin is one of the most abundant and highly conserved

intracellular protein in eukaryotes, with only a few amino acids sequence differences between distant evolutionarily species, like humans and slime molds (Wagner *et al*., 2002). Actin is found in two main states: globular actin (G-actin) a monomeric form, with about 42kDa, and filamentous actin (F-actin) a helical polymer (Reisler and Egelman, 2007). G-actin has the ability to polymerize into F-actin and F-actin to depolymerize into G-actin. Actin filaments are polarized structures (Yamasaki, 2005) with a fast-growing end or barbed end, where actin monomers are preferentially incorporated, and a slow-growing end or pointed end, where actin filaments are disassembled by loss of monomers (Cooper, 2000). This is an ATP dependent process, called treadmilling (schematized in Fig. 1.9).

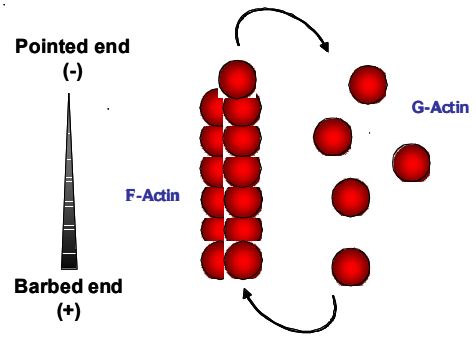

Figure 1.9 – Process of treadmilling. Actin monomers are incorporated at the barbed end, while disassemble from the pointed end.

The polarized actin cytoskeleton is a key feature of epithelial cells. As it has already been mentioned, a continuous band of actin filaments (localized apically) links epithelial cells to each other, forming the zonula adherens (ZA). This structure, called actin belt, is extremely important for the maintenance of epithelia, since it provides adhesive strength between epithelial cells (Baum and Perrimon, 2001). This structure is formed from actin bundle arrangements and is composed of cortical actin filaments that encircles the cell together with the adherens junctions (Abe and Takeichi, 2007). In addition, non-muscle cells contain stress fibres localized at the basal sites. Stress fibers are bundles of actomyosin that are the major mediators of cell contraction and allow cells to respond to imposed mechanical force with a bracing resistance (Pellegrin and Mellor,

2007).

The actin cytoskeleton forms and maintains morphological features in differentiated cells that correlate with their specialized functions. These features include membrane protrusions such as microvilli, bristles, filopodia and lamellipodia. Microvilli structures are observed in the thorax of *Drosophila* and are involved in mechanosensing. In *Drosophila*, bristles are actin based structures that have sensory function. Lamellipodia and filopodia are membrane extensions at the leading edge of cells which formation is involved in either motility or interactions with other cell types (Revenu, 2004). The most common F-actin arrangements in these different membrane structures occur in different forms: as cortical actin found in all cells and as bundled or branched assemblies (Fig. 1.10) (Röper *et al*., 2005). Functionally, bundles and networks (branched actin) have identical roles in a cell: both provide a framework that supports the plasma membrane and, therefore, determines a cell's shape. Structurally, bundles differ from networks mainly in the organization of the actin filaments. In bundles the actin filaments are closely packed in parallel arrays, whereas in a network the actin filaments criss-cross, often at right angles, and are loosely packed (Winder and Ayscough, 2005). The actin framework formed, whether in bundles or networks, depends on what actin binding proteins (ABPs) are associated to the F-actin.

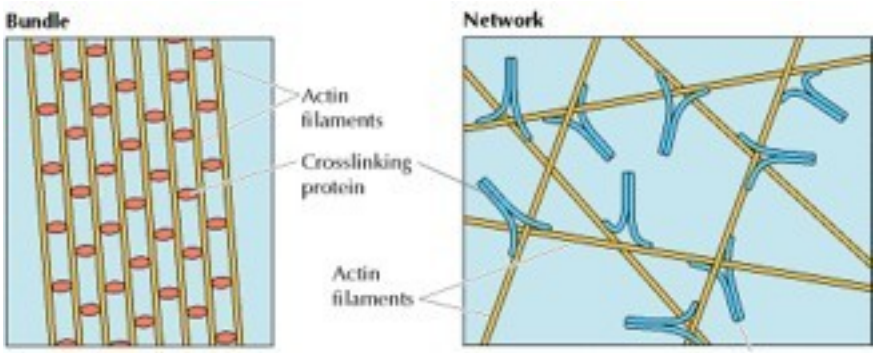

Figure 1.10 – Schematic organization of actin bundles and networks. Actin filaments in bundles are crosslinked into parallel arrays by small proteins that align the filaments closely with one another. In contrast, networks are formed by large flexible proteins that crosslink orthogonal filaments (Cooper, 2000).

Cell protrusions are important for the growth and patterning of tissues and organs

since they may mediate intercellular communication (Marzesco *et al*., 2005). Some protrusions have been described also in the wing imaginal discs. The apical side of imaginal discs is decorated with microvilli (Ursprung, 1972), while filopodia are present at their basal side (Eaton *et al*., 1995). Also, cells at the periphery of the columnar cell sheet have long, planar filopodia-like protrusions, called cytonemes (Ramirez-Weber and Kornberg, 1999).

2.1 – Like in Vertebrates, *Drosophila* contains six actin genes

There are many fundamental similarities in the biology of *Drosophila* and vertebrates. Most of higher organisms contain multiple actin genes. For instance, humans, mice and flies have six actin genes (Röper *et al*., 2005). In *Drosophila*, Actin protein is encoded by: *actin5C*, *actin42A*, *actin57B*, *actin79B*, *actin87E* and *actin88F* genes. *Drosophila* actin genes can be subdivided into 3 groups, based on the developmental stage where they are expressed (Fyrberg *et al*., 1983). Two actin genes encode cytoplasmic actins (*actin 5C and 42A*), while four encode muscle-specific actin isoforms. The four muscle actins can be further subdivided into flight muscle actins (*actin 79B and actin 88F*) and larval muscle actins (*actin 57B and actin 87E*) (Fig. 1.11) (Fyrberg *et al*., 1983). All six *Drosophila* actins are more closely related to vertebrate cytoplasmic actins than to any of the muscle-specific vertebrate actins, with the two fly cytoplasmic actins being the most similar to the two vertebrate cytoplasmic actins (Fig. 1.11).

Throughout this work and accordingly to the available literature the term actin genes and actin isoforms will be used to design the same concept. However, it is important to notice that by using actin isoform we do not refer to protein isoforms that come from a unique gene but rather the 6 actin proteins which derive from 6 independent genes.

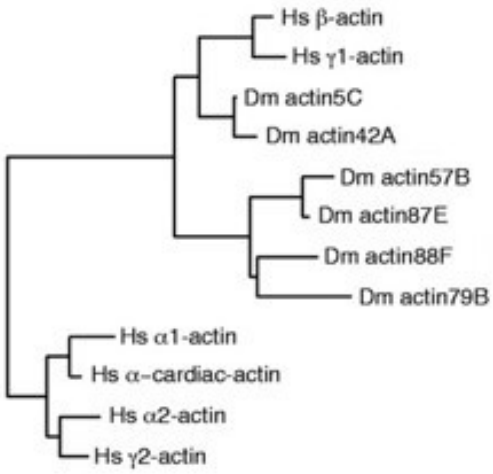

Figure 1.11 – Phylogenetic relationship between all fly and human actin genes (Röper *et al*., 2005). All fly actins are more closely related to vertebrate cytoplasmic actins than to vertebrate muscle actins.

Within species and even between distant species like fly and human, the actin proteins differ from each other in only a few aminoacids (Fig. 1.12) (Röper *et al*., 2005). In *Drosophila melanogaster*, the six actin genes encode proteins whose aminoacids sequences share greater than 85% homology (Tobin *et al*., 1980; Fyrberg *et al*., 1981; Sanchez *et al*., 1983). This high conservation observed at the protein level raises an interesting question: what is the reason for the existence of multiple actin genes and why they have been retained through evolution.

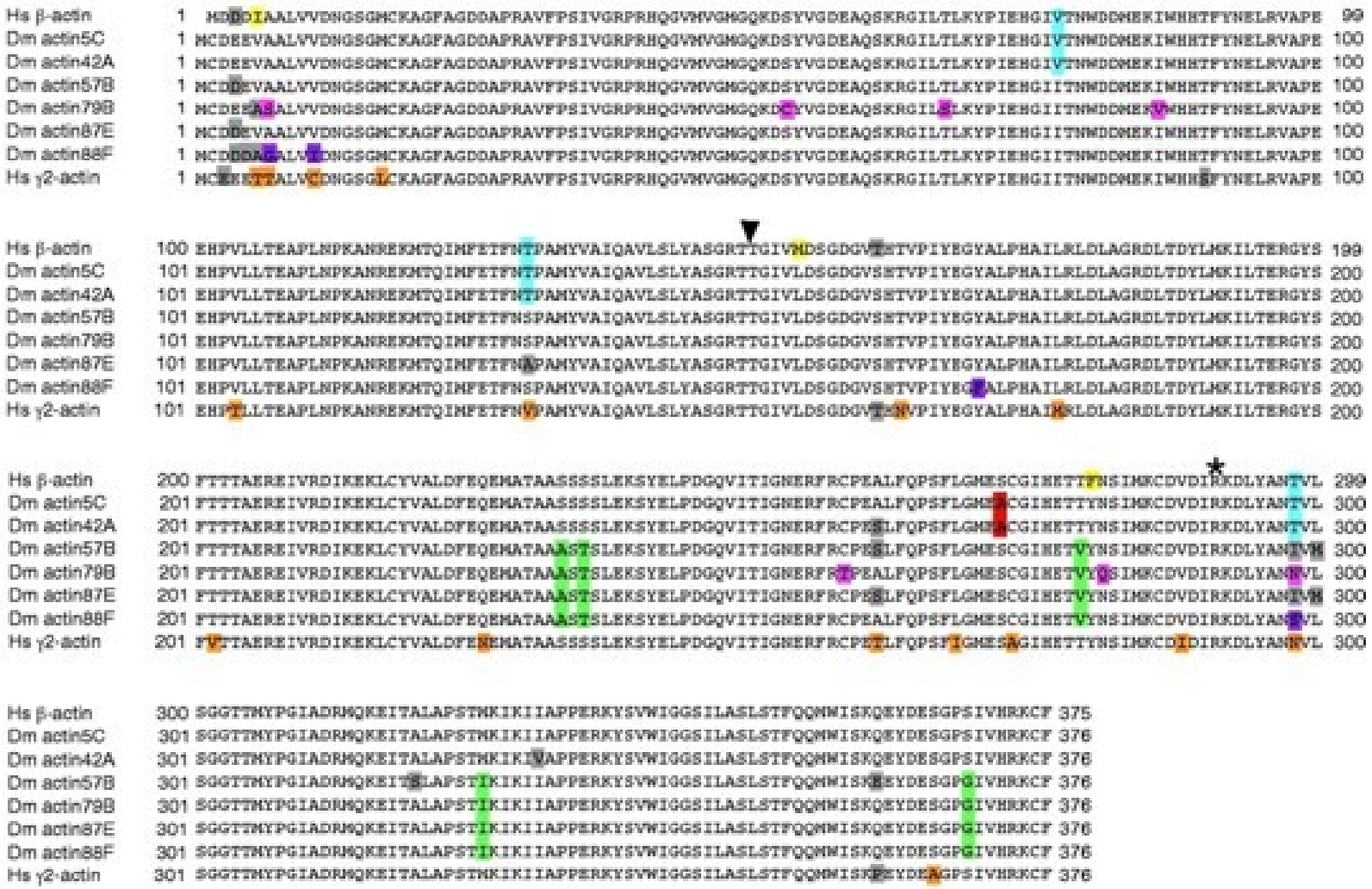

Figure 1.12 – Sequence alignment of the six *Drosophila* and two human actin proteins (Röper *et al*., 2005). Colors indicate residues conserved between groups of actins in flies or human: blue indicates cytoplasmic actin-specific residues; red indicates residues specific to fly cytoplasmic actins; yellow, human cytoplasmic actins; green, fly muscle-actins-specific residues; pink and purple, residues specific for actin 79B and 88F, respectively; orange, human muscle-specific residues; grey, all other non-conserved residues.

2.2 – Actin "isoforms" are highly regulated

Although actin protein sequences are very similar, each actin gene exhibits a unique profile of transcript accumulation throughout development (Fyrberg *et al*., 1983; Sanchez *et al*., 1983), suggesting that they have evolved independent regulatory programs (Vigoreaux and Tobin, 1987). In fact, actin genes have several levels of regulation (Fyrberg *et al*., 1983; Röper *et al.*, 2005).

2.2.1 – Actin genes are regulated at a transcription level

The first level of regulation of actin genes is at the transcription level. For instance, when fragments of cloned actin genes were used to examine the levels of individual mRNAs in different developmental stage organisms and dissected body parts, it was found that each actin gene is transcribed to form functional mRNA, which accumulates with a distinct pattern (Fyrberg *et al*., 1983). The timing of mRNA expression of actin genes during development of *Drosophila* shows that for the larval muscle actins, the actin 57B mRNA is expressed during embryogenesis and larval stages and actin 87E mRNA is expressed throughout life. The flight muscle actins 79B mRNA and 88F mRNA are mostly expressed during pupal and adult stages. For the two cytoplasmic actin, although actin 5C mRNA is expressed throughout life, actin 42A mRNA is mostly expressed during embryonic and pupal stage (Fyrberg *et al*., 1983). These observations suggest a temporal expression restriction. In addition, within specific tissues each actin gene mRNA seems to be spatially restricted. For instance, actin 57B mRNA and 87E mRNA are transcribed in the body wall muscle; actin 79B mRNA in the wing, thorax and leg muscle, while, actin 88F mRNA is transcribed in the indirect flight muscle (Fyrberg *et al*., 1983). So, at the transcriptional level, mRNA expression is restricted at both, temporal and spatial expression patterns (Fig. 1.13A) (Fyrberg *et al*., 1983). In wing imaginal discs, the actin 57B mRNA is expressed in the wing notum at third instar larvae but not in the wing hinge or blade (Fig. 1.13B), whereas nothing is known about expression pattern of the rest of the actin genes.

The second level of actin genes regulation is the alternative splicing (FlyBase). In addition, actin production at specific locations within a cell can also be regulated, by actin mRNAs subcellular localization. For instance, the lethal mutation of cytoplasmic actin 5C gene can be rescued by reintroducing the protein-coding region of the other cytoplasmic actin 42A gene, under the control of the regulatory regions of the actin 5C (Wagner *et al*., 2002). This indicates that the amino acids differences between these two cytoplasmic actin isoforms are not important for function, suggesting that it is the regulated expression of actin 5C gene that is essential for the fly (Wagner *et al*., 2002). However, another study showed that flightless flies, which resulted from null mutations in a flight muscle actin gene, the actin 88F gene, could not be rescued by other types of actin genes, cytoplasmic or larval (Fyrberg *et al.*, 1998).

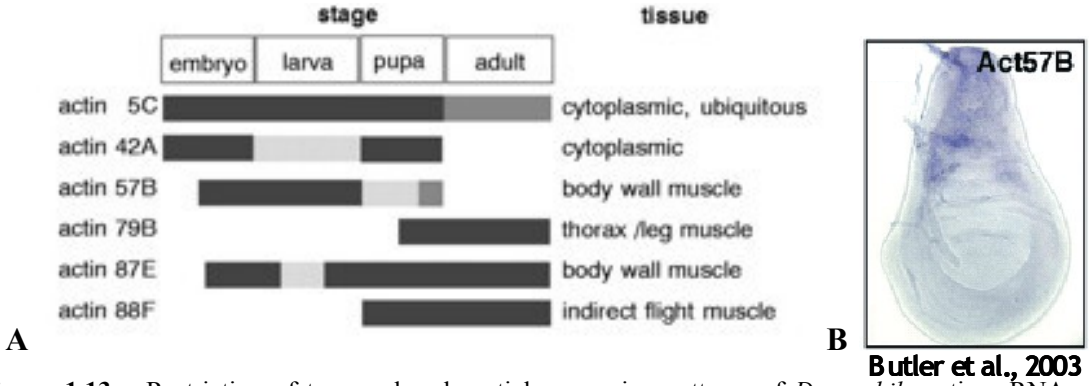

Figure 1.13 – Restriction of temporal and spatial expression patterns of *Drosophila* actin mRNAs. (A) Diagram of the timing of expression of the six actin mRNAs during *Drosophila* development using northern blot analysis (Fyrberg *et al*., 1983). White boxes equal no expression, and the darker the boxes are shaded, the higher the expression level is (Röper *et al*., 2005). (B) Expression pattern of actin 57B mRNA in third instar wing imaginal disc (Butler *et al.*, 2003). Note that actin 57B might be more strongly expressed in the wing notum region of the disc.

2.2.2 – Actin genes might be regulated at a post-translational level

The different actin genes might also be regulated at the protein level (Röper *et al*., 2005). When actin-GFP fusion proteins are overexpressed in *Drosophila* follicular epithelium, they are incorporated in different actin filament structures within the cell. For

instance, actin 5C and 42A incorporate strongly in stress fibers while actin 57B is more cortical, being weaker in that cellular structure (Fig. 1.14) (Röper *et al*., 2005). In addition, some ABPs interact more efficiently with specific actin filament structures, like the mammal β-cap73 that prevents polymerization of the β-filamentous actin but not the α-filamentous actin (Welch and Herman, 2002). Another ABP, Ezrin in vertebrates, also interacts specifically with β-actin but not with the α-actin filaments (Shuster and Herman, 1995). These experiments strongly support the idea that the different actin isoforms might have specialized functions.

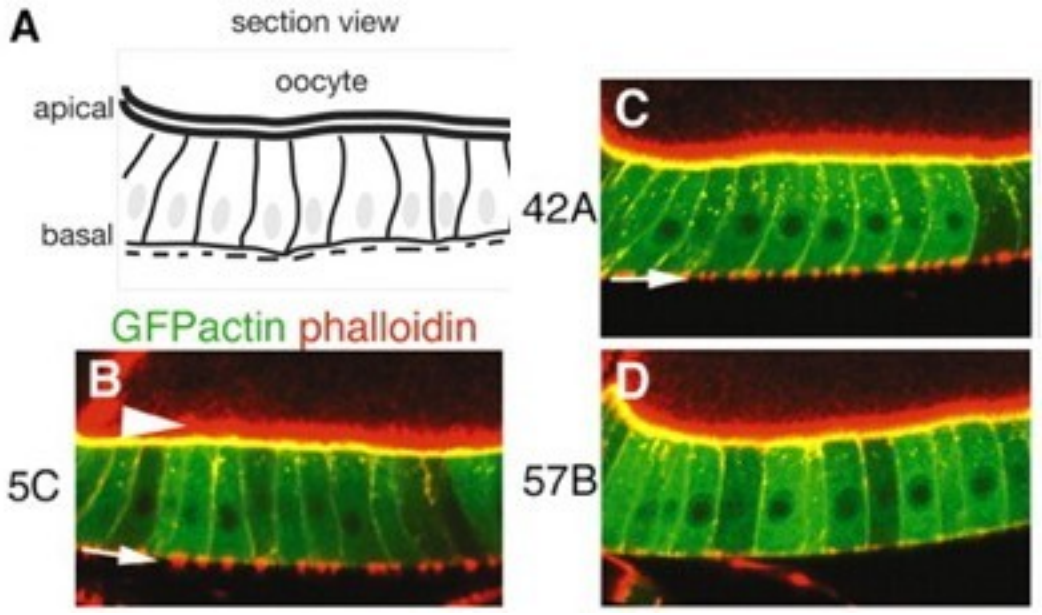

Figure 1.14 – Actin genes incorporate into different actin filaments structures in the *Drosophila* follicle epithelium (Röper *et al*., 2005). (A) Diagram illustrating the follicle epithelium. (B-D) Confocal sections through the epithelium, overexpressing fusion proteins between GFP and *actin 5C* (*act 5C-GFP*) (B), *42A (act 42A-GFP)* (C) or *57B (act 57B-GFP*) (D). Egg chambers are stained with Phalloidin in red, which stain actin filaments and with an anti-GFP antibody. Note that Act 42A-GFP and Act 5C-GFP incorporate more strongly in stress fibers (white arrow), while Act 57B-GFP incorporate strongly in cortical filaments.

There are several possible reasons why organisms have multiple, highly similar actin genes. One explanation is, the organisms need a large quantity of actin, and the best

way to supply enough actin may be to have multiple genes. In this case, the amino acid sequence differences between the actin genes would have no functional consequences. Another reason could be, some cells need more actin than others and by having multiple genes provides a mechanism for differential regulation of actin expression. In this case, the amino acid differences would not be functionally significant either, but the regulation of the expression of genes would be critical. Finally, a strong reason could be, the small number of amino acid sequence differences may be functionally important. These differences might allow different genes to have different roles within the same cell (Wagner *et al*., 2002). For instance, it was demonstrated recently, that each actin gene, in *Paramecium tetraurelia*, plays a role in a different cellular mechanism (Sehring *et al.*, 2006). Moreover, some actin genes act in cell division, while others act in vitality, cell shape or swimming behavior.

3 – The dynamic of the actin cycle is regulated by Actin Binding Proteins

Most cells control the length, number and distribution of actin filaments under conditions where total actin concentration remains approximately constant (reviewed in Dos Remedios *et al*., 2003). Actin filament growth, assembly and disassembly, and also, their organization into functional higher-order networks are known to be controlled by many actin binding proteins (ABPs) (Winder and Ayscough, 2005). Actin binds approximately 162 distinct and separate ABPs. At least 12 ABPs are membrane-associated proteins and another 9 are membrane receptors or ion transporters. About 13 ABPs cross-link actin filaments, while others enable filaments to interact with other elements of the cytoskeleton. In addition, actin binds 30 other ligands including drugs and toxins (reviewed in Dos Remedios *et al*., 2003).

3.1 – The Actin Binding Proteins

Dos Remedios classified the ABPs into seven groups, according to their function in the actin cycle. Monomer-binding proteins sequester G-actin and prevent its polymerization (e.g., thymosin β4 and DNaseI); Filament-depolymerizing proteins induce the conversion of F-actin to G-actin (e.g., CapZ and cofilin); Filament end-binding proteins cap the ends of the actin filament preventing the exchange of monomers at the pointed end (e.g., tropomodulin) and at the barbed end (e.g., CapZ); Filament severing proteins shorten the average length of filaments by binding to the side of F-actin and cutting it into two pieces (e.g., gelsolin); Cross-linking proteins contain at least two binding sites for F-actin, thus facilitate the formation of filament bundles, branching filaments, and three-dimensional networks (e.g., Arp2/3); Stabilizing proteins bind to the sides of actin filaments and prevent depolymerization (e.g., tropomyosin); Motor proteins use F-actin as a track upon which to move (e.g., the myosin family of motors). However, it is important to note that, ABPs are not limited to one class. For instance, gelsolin is capable of severing and capping the barbed end of actin filaments, and the Arp2/3 complex can nucleate filament formation, elongate filaments, and establish branch points in actin networks (reviewed in Dos Remedios *et al*., 2003). With such a broad and important function, ABPs are an appealing group of proteins to analyze to gain some insights on the final function of the actin cytoskeleton.

3.2 – Capping protein: a highly conserved heterodimer

One interesting ABP is capping protein (CP). *In vitro* studies showed that CP binds the barbed end of actin filaments through the C-terminal region of both units (Wear and Cooper, 2004), preventing the addition or loss of actin monomers (Schafer et al., 1995). The barbed end of F-actin has higher rates of association and dissociation with G-actin and a lower critical concentration for polymerization of actin than the pointed end. CP together with Arp2/3 complex, which promotes filament branching, favors the

formation of the short highly branched actin filaments required to generate protrusive force at the leading edge of migrating cells (Fig. 1.15) (Bear *et al*., 2002).

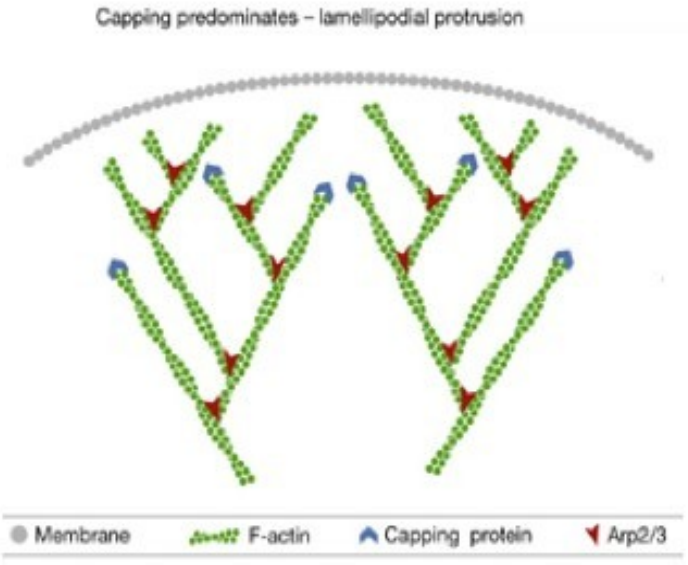

Figure 1.15 – CP together with Arp2/3 complex favors the formation of the short highly branched actin filaments (adapted from Ayscough and Winder, 2004).

All together, the mechanism and regulation of CP have been studied, most of the available data results from in vitro biochemical studies and cells in culture. Since these analyses can be incomplete since *in vitro* analysis not exactly reproduce the *in vivo* complexities within a tissue (Hopmann and Miller, 2002), it is important to understand the role of CP and its regulation within a tissue.

In *Drosophila*, CP is a highly conserved and ubiquitous heterodimer of two protein subunits, each approximately of 30 kDa, encoded by the *capping protein* α and the *capping protein* β genes (Hart *et al*., 2000). Up to date, mutations in either of these genes give the same phenotype (Hopmann and Miller, 2003). Null mutations genes are lethal, but partial loss of function alleles are viable (Hopmann and Miller, 2003).

3.3 – *In vivo* studies with capping protein

As previously proposed by *in vitro* studies, clonal analysis in the *Drosophila* wing imaginal disc showed that CP is required for the prevention of actin filaments polymerization. In this study, the *cpa* mutation increase actin filament polymerization (Janody and Treisman, 2006). Interestingly, CP doesn't have the same developmental function in all epithelia. It was observed that, loss of *cpa* leads to accumulation of actin filaments in different regions of the wing disc. In the wing blade epithelium the actin filaments accumulate around the entire cell cortex, while in the notum and hinge, the actin filaments accumulate in the apical regions of cells (Fig. 1.16).

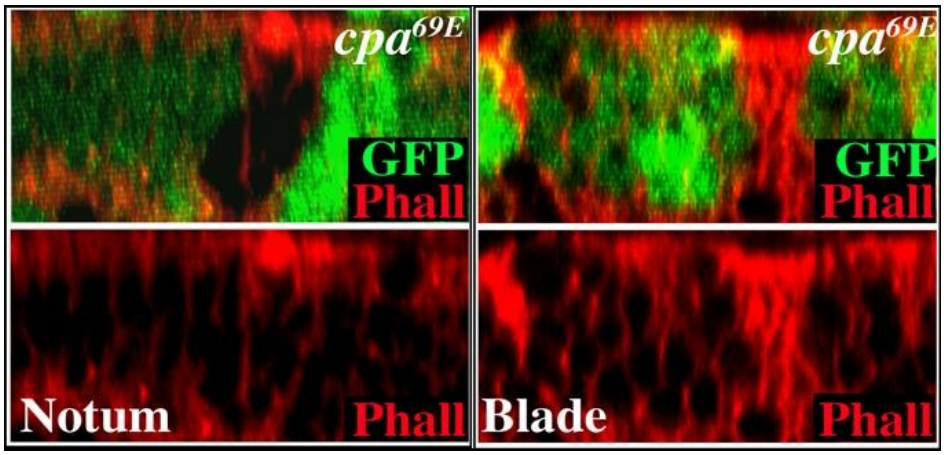

Figure 1.16 – Loss of *cpa* leads to accumulation of actin filaments in different regions of the wing disc (adapated from Janody and Treisman, 2006). Optical cross sections through *Drosophila* third instar wing imaginal disc, comparing the notum and blade regions. The clones are negatively marked by GFP and discs are stained with Phalloidin to reveal F-actin (red).

Also, in other study, it was demonstrated that loss of function of CP increases the amount of F-actin in *Drosophila* bristles (Hopmann and Miller, 2003). As already mentioned, *Drosophila* bristles are actin based structures that serve for the sensory function. Interestingly, CP seems to prevent polymerization of only a subpopulation of actin filaments within the bristles (Frank *et al*., 2006). CP does not primarily act directly on actin bundles, but rather on a dynamic population of actin filaments that are not part of

the bundles, the actin snarls.

Clonal analysis in the *Drosophila* wing imaginal disc epithelium revealed a new feature of CP. They are required for the maintenance of cells within the wing blade epithelium (Janody and Treisman, 2006). This is because, mutant cells for either *cpa* or *cpb* in these region suffer basal extrusion and apoptosis (Fig. 1.17). Interestingly, the requirement for CP to maintain cells within the epithelia is restricted to the wing blade region, since cell extrusion and death caused by loss of CP occurred exclusively in the blade but not in the hinge and notum regions.

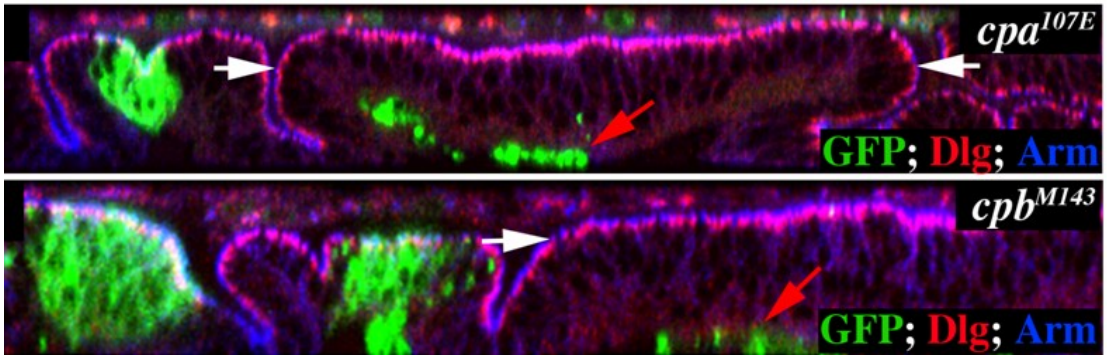

Figure 1.17 – Clones of mutant cells for *cpa* and *cpb* extrude from the wing blade epithelium (adapted from Janody and Treisman, 2006). Optical cross sections through the wing disc epithelium. Mutant clones are marked positively by GFP (green) and discs are stained with anti-Dlg (red) and anti-Arm (blue) to outline apical membranes. The wing blade region is indicated with white arrows.

data). The scalloped driver is express broadly in 1st instar imaginal wing imaginal discs and this expression gets restricted mainly to the pouch region (Janody, unpublished data). In this experiment, although some *cpb*-depleted cells expressed activated Caspase 3, most of the cells were able to survive and overproliferate. However, this was not observed in *cpb* mutant clones (Fig. 1.17). In a clonal situation, the mutant cells extruded basally and died as already discussed. All together this data may suggest that *cpb* mutant clones dye probably due to a cell competition effect, since the *cpb* mutant cells behave differently, depending on the local environment, in small groups of cells or when the whole tissue is affected.

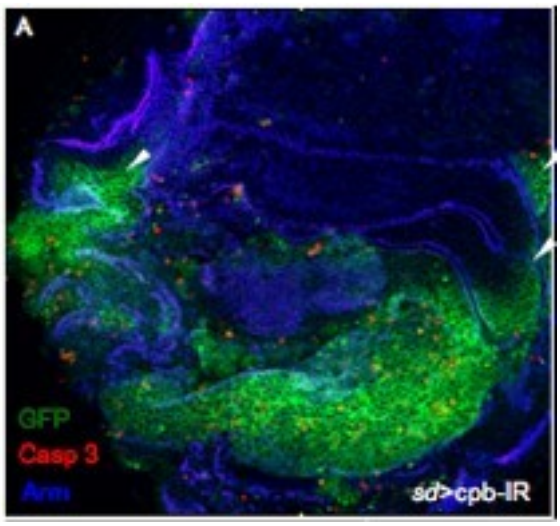

Figure 1.18 – Broad deplection of *cpb*, targeted to *sd*-expressing cells, leads to overgrowth (adapted from Rebelo, unpublished). Standard optical section shows third instar wing imaginal disc marked with GFP (green) and stained with anti-Arm (blue) and anti-activated Caspase 3 (red). (A) *cpb* depletion with the *scalloped* driver, leads to overgrowth and cell migration.

II – Aims

Like in mammals, *Drosophila* has six actin genes, closely related to vertebrate cytoplasmic actins. Even though all fly actins are closely related, functional substitution tests have shown that some can compensate for loss of another actin while others cannot (Fyrberg *et al.*, 1998; Wagner *et al*., 2002). This data suggests that actin genes are not functionally equivalent. For instance, the deleterious lack of cytoplasmic actin 5C can be rescued by reintroducing the coding sequence of the other cytoplasmic actin, actin 42A, under the regulatory control of actin 5C elements (Wagner *et al*., 2002). By contrast, lack of the indirect flight muscle-specific actin 88F cannot be rescued by expression of other types of actin genes, cytoplasmic or larval (Fyrberg *et al*., 1998). Also, all actins genes promote excessive actin filaments polymerization when overexpressed, but each actin seems to incorporate more efficiently in specific actin structures (Röper *et al*., 2005), suggesting that they promote different cytoskeleton structures. Despite this data, it is still not clear, the reason for the existence of multiple actin genes.

Some ABPs regulate specific actin filaments in mammals (Welch and Herman, 2002; Shuster and Herman, 1995), therefore, it may be possible that CP might prevent polymerization of specific actin isoforms to maintained cells within the epithelium.

The main goal of this work is to determine if the phenotype observed when the CP is depleted, which is the extrusion and death of wing blade cells, is a consequence of excessive actin filaments accumulation. To confirm this, it is necessary to test whether the overexpression of any specific actin isoform gives a similar phenotype to the loss of CP. To do so, I analyse here the developmental consequences of overexpressing each of the six actin genes during epithelial morphogenesis. As a model system I will use the epithelium of the wing imaginal discs of *Drosophila's* third instar larvae.

In this work I will overexpress all the six *Drosophila* actin genes fused to GFP using the UAS-Gal4 system and the Gal80 system to drive expression in wing imaginal discs.

III – Materials and Methods

1 – Fly strains and genetics

1.1 – Methods of culturing flies

Fly stocks can be successfully cultured by periodic mass transfer of adults to fresh food in bottles or vials. Since temperature has a large effect on the rate of *Drosophila* development, flies were raised at 25ºC (unless otherwise indicated) and the crosses were cultured in small vials, under standard conditions. Virgin females are required for successful crosses; *D. melanogaster* adults do not mate for about 10h after eclosion, allowing virgins to be collected within 8-12h after the culture was cleared of adults (reviewed in Roberts, 1998).

1.2 – Genetics tools

1.2.1 – Fly stocks

Table 3.1 – Fly stocks used for the overexpression experiments of the different actin genes.

UAS lines	**References**
UAS-actin5C-GFP (2-1)	Verkhusha *et al*., 1999
UAS-actin42A-GFP (5-5)	Röper *et al.*, 2005
UAS-actin57B-GFP (6-1)	Röper *et al*., 2005
UAS-actin79B-GFP (3-1)	Röper *et al*., 2005
UAS-actin87E-GFP (7-6)	Röper *et al*., 2005
UAS-actin88F-GFP (15-1)	Röper *et al*., 2005
Drivers	**References**
FRT40 or 42D Gal80	Lee and Luo, 2001
nubbin-Gal4 (*nb*-Gal4)	Thompson and Cohen, 2006
daughterless-Gal4 (*da*-Gal4)	Wodarz *et al*., 1995
engrailed-Gal4 (*en*-Gal4)	Brand and Perrimon, 1993
scalloped-Gal4 (*sd*-Gal4)	Willert *et al*, 1999

1.2.2 – The FLP/FRT system

To generate mitotic clones usually the FLP/FRT system is used (Fig. 3.1). In a heterozygous parental cell, the site-specific recombinase FLP induces mitotic recombination between FRT sites on homologous chromosome arms. The FLP is expressed under the control of a heat shock promoter. Segregation of recombinant chromosomes at mitosis produces two daughter cells: a mutant cell bearing two copies of the mutant allele and a wild type cell containing only the wild type form of the gene (reviewed in St. Johnston, 2002).

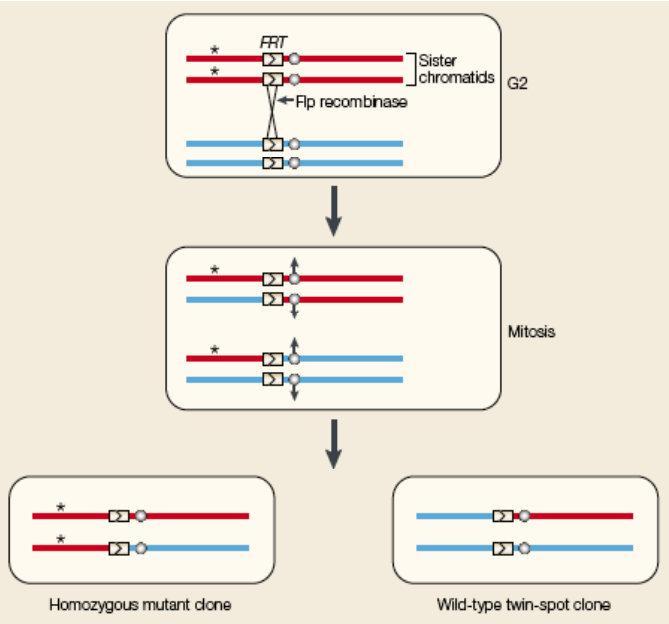

Figure 3.1 – The FRT/FLP system (reviewed in St. Johnston, 2002).

2002)

1.2.3 – The use of the UAS-Gal4 System

The UAS-Gal4 system (Fig. 3.2) allows the selective expression of any cloned gene in a wide variety of cell and tissue specific patterns in *Drosophila*. A promoter directs expression of the transcriptional activator Gal4, and this in turn directs transcription of the Gal4 responsive UAS target gene. The Gal4 gene and the UAS target are initially separated into two distinct transgenic lines. In the Gal4 line, the activator protein is present, but has no target gene to activate. While in the UAS target gene line, the target gene is silent because the activator is absent. It is only when the Gal4 line is

crossed with the UAS target gene line that the target gene is turned on its progeny (reviewed in St. Johnston, 2002).

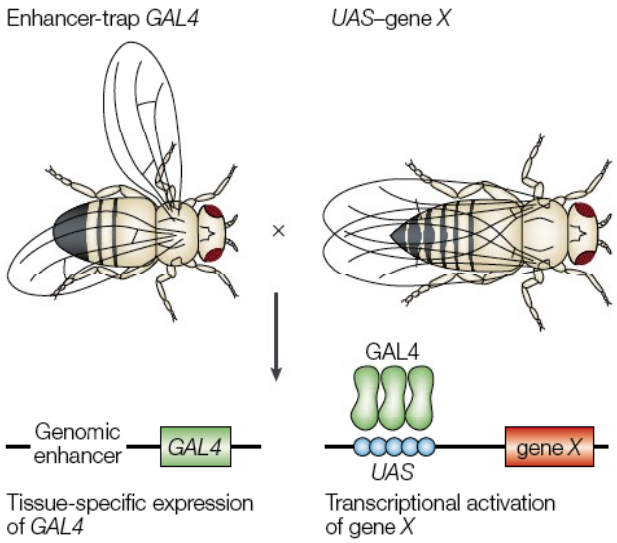

Figure 3.2 – The UAS-Gal4 system (reviewed in St. Johnston, 2002).

To drive the expression of each actin-GFP fusion gene in restricted expression domains in the wing imaginal disc, males carrying either one of the actin isoforms (see Table 3.1) were crossed with transgenic females bearing the following promotors: *nb*-Gal4, *en*-Gal4, *sd*-Gal4 or *da*-Gal4.

1.2.4 – The use of the MARCM system

The Gal80 system is based in a Gal4 inhibitor, the Gal80, which provides a way of controlling the UAS-Gal4 system (Lee and Luo, 1999). When Gal80 expression is driven with a tubulin promoter (tub-Gal80), it can inhibit the activity of a tubulin promoter-Gal4 construct. If Gal80 is removed, Gal4 is activated and drives the expression of a UAS construct. In the MARCM (Mosaic Analysis with a Repressible Cell Marker) technique (Fig. 3.3), the tub-Gal80 is removed using FRT mediated mitotic recombination (Lee and Luo, 1999). By this system the clones are marked positively

(Brumby and Richardson, 2005).

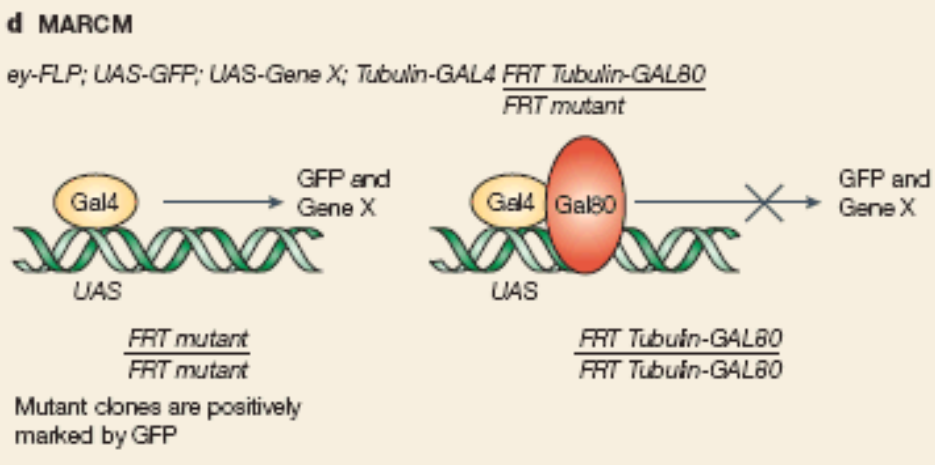

Figure 3.3 – The MARCM system (adapted from Brumby and Richardson, 2005).

To generate clones marked positively by GFP in the wing imaginal disc, $y^{-}w^{-}$; FRT42D, UAS-actin5C-GFP/CyO,y^{+} or $y^{-}w^{-}$; FRT40, UAS-actin42A-GFP or UAS-actin57B-GFP or UAS-actin79B-GFP or UAS-actin87E-GFP or UAS-actin88F-GFP/CyO,y^{+} males were crossed with $y^{-}w^{-}$; *hs*FLP_{122}, UAS-GFP; FRT40 or 42D, *tub*-Gal80; *tub*-Gal4/TM6B virgin females. To induce clones by using this system, the progeny was heat-shocked for 50min at 37ºC, 24 and 48hs after overnight collection, corresponding to the 1st and 2nd instar larvae (Fig. 3.4).

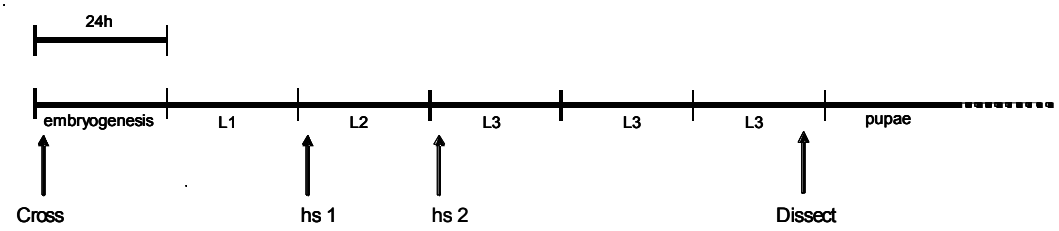

Figure 3.4 – Time course of *Drosophila* development and the methodology used for clone induction. L1, L2 and L3 correspond to 1st, 2nd, 3rd instar larvae, respectively. hs: heat shock.

2 – Western blot

2.1 – Embryos extract

To compare the level of overexpression of the six UAS-actin transgenes fused to GFP, $y^{-}w^{-}$; FRT42D, UAS-actin5C-GFP/CyO,y^{+} or $y^{-}w^{-}$; FRT40, UAS-actin42A-GFP or UAS-actin57B-GFP or UAS-actin79B-GFP or UAS-actin87E-GFP or UAS-actin88F-GFP/CyO,y^{+} males were crossed with virgin females carrying the ubiquitous *da*-Gal4 driver. The six crosses, in addition to a control $y^{-}w^{-}$ line, were left to lay overnight on apple juice plates. Embryos were collected the following day under a GFP stereoscope to select embryos that expressed GFP. Embryos were then washed, immerged in bleach 100% for 5min to remove the chorion and washed thoroughly. Ten embryos were placed in a solution of 10µl 1:1 of SDS loading buffer/PBS. Extracts were kept at -20ºC before using.

2.2 – SDS-PAGE/Gel preparation

Before loading to a 12% polyacrylamide gel (30% acrylamide, Tris pH 8.8, 10% SDS, 10% APS and TEMED) covered by a stacking gel (30% acrylamide, Tris pH 6.8, 10% SDS, 10% APS and TEMED), samples were boiled for 5min, cooled down on ice and centrifuge for 1min at maximum speed. 5µl of embryonic extracts were used for loading. Electrophoresis was performed at 125V in running buffer (144g of glycine, 30g of Tris, 25ml of SDS 20% and H_2O per liter).

2.3 – Proteins transfer to PVDF membrane

Following electrophoresis, the polyacrylamide gel was equilibrated in transfer buffer (Tris 480mM and glycine 390mM, 100% methanol, 10% SDS) for 20min. The PVDF membrane was treated with methanol for 10s, washed with water for 5min and equilibrated in transfer buffer for 10min. The transfer cassette was prepared as follows: 1 sponge, 2 Whatman papers, gel, membrane, 2 Whatman papers and 1 sponge. The transfer was done at 100V for 1h with agitation.

2.4 – Membrane staining

To make sure that total proteins were correctly transferred, the membrane was stained with a Ponceau S solution 1 % (w/v) in 5% acetic acid for 5min, then washed for 2min with water and for 20min with PBS, then blocked with 10% milk in PBST (PBS with 0,1% Tween 20) for 1h at room temperature (RT) with agitation to avoid unspecific binding of the antibody and washed again in PBST. The membrane was cut into two pieces, separating the actin-GFP bands from the loading control bands, and each of them were incubated for 1h at RT with shaking with the primary antibodies, diluted in 1% milk in PBST. The rabbit anti-GFP antibody (1:20000; Invitrogene), which recognizes each of the Actin-GFP fusion protein, was applied to the membrane containing proteins of high molecular weight, while the rabbit anti- β3-tubulin antibody (1:2000; Sigma), which reveals the quantity of protein for each extract, was applied to the membrane containing proteins of low molecular weight. Both membranes were then washed with PBST, and in PBST 5% milk and then incubated with the secondary antibody, anti-rabbit peroxidase conjugated with HRP (1:10000; Jackson Immunoresearch) in 1% milk in PBST. The incubation was performed in the dark and as described previously for the primary antibody. The membranes were then washed in PBST 3 times for 15min and washed in PBS for 15min. The kit ECL Plus Western Blotting Detection System (Amersham) was used to reveal the PVDF membrane. According to the kit instructions, a mix of solution A with solution B was added to the membrane for 5min. Storm equipment was used to scan the membrane. The intensity of the bands was quantified using the ImageJ programme.

3 – Immunohistochemistry

3.1 – Antibody staining

Third instar larvae wing imaginal discs were dissected in 0,1M phosphate buffer pH 7,2 (72% Na_2HPO_4 0,5M and 28% NaH_2PO_4 1M) and fixed in 4% formaldehyde (FA) in PEM 2x (0,1M PIPES pH 7,0; 2mM $MgSO_4$; 1mM EGTA) for 30min on ice. Discs were then washed in PBS 0,2% Triton (PBT) for 15min and incubated with the primary antibodies in PBT 10% Donkey serum overnight (ON) at 4ºC. The primary antibodies used in this work were a mouse anti-Armadillo (1:10; Hybridoma Bank) which marks adherens junctions and a rabbit anti-activated Caspase 3 (1:50; Cell Signaling Technology) which stains Caspase-dependant apoptotic cell death. Discs were then washed 3 times for 10min in PBT and incubated in the dark with the secondary antibodies in PBT 10% donkey serum for 2h at 4ºC. Secondary antibodies were an anti-mouse and an anti-rabbit conjugated to TRITC and Cy5 respectively (1/200; Jackson Immunoresearch). Imaginal discs were washed again 3 times for 10min with PBT before mounting between slides and coverslides in Vectashield medium (Vector Laboratories). Fluorescence images were obtained on a LSM 510 Zeiss Meta confocal microscope. In figures, the wing blade and hinge regions size were delimitated by measuring the distance between blade and hinge folding based on the Armadillo staining alone.

3.2 – Phalloidin staining

Third instar larvae wing imaginal discs were dissected and fixed as described in the previous section. This procedure was followed by incubation with Rhodamine-conjugated Phalloidin (Sigma), which stains F-actin, for 4min at 4ºC in the dark. Phalloidin was diluted in PBT 10% donkey serum and used at a concentration of 1:200. Mounting of the wing imaginal discs and image acquisition were performed as previously described.

4 – Molecular biology

In order to determine the expression pattern of each actin isoform in the wing imaginal discs, I used common molecular biology techniques to create specific actin RNA probes. The cDNA sequences of the six actins are more or less 85% homologous to each other, while untranslated regions, comprising the 3'UTR are divergent (Fyrberg *et al*., 1981). RNA probe, generated against the entire cDNA of one particular actin will likely cross hybridize with all other actin RNA. Therefore, in order to generate RNA probes that recognizes specifically each actin isoform. I used the most divergent cDNA fragments for each gene, comprising the 3'UTR untranslated sequences, to subclone. The selected subcloned fragments and their sizes are represented in Fig. 3.5.

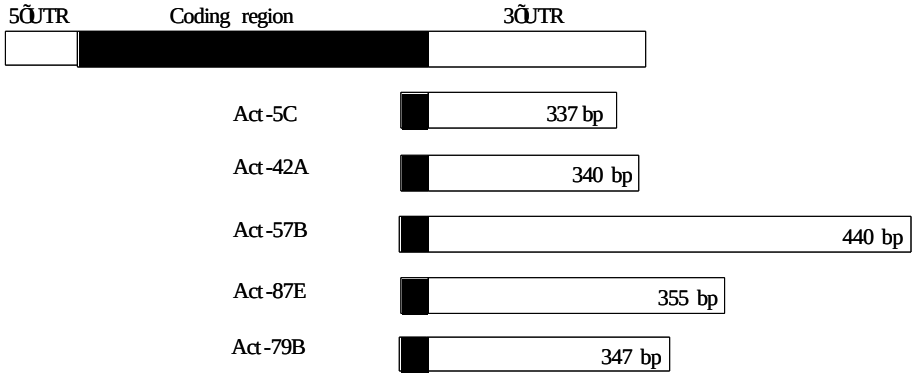

Figure 3.5 – Representative diagram of transcribed region of each actin gene. In black is the coding region. In white is represented the 3'UTR, the selected fragment used to subclone (adapted from Fyrberg *et al*.,1983).

The probe for the actin 88F gene was not made because there was not any cDNA clone available at the *Drosophila* Genomics Resource Center (DGRC).

4.1 – Classical techniques of Molecular Biology used in this study

4.1.1 – Preparation of competent cells

A pre-culture of DH5α cells was grown in LB medium, ON at 37ºC and inoculated the following day to a large volume of LB medium. The culture was incubated at 37ºC until the OD_{600} reached a density of 0,5. The culture was then placed on ice for 10min and centrifugated for 10min at 4ºC. The pellet was resuspended in a 100mM $CaCl_2$ solution and incubated on ice for 20min, centrifugated again for 10min at 4ºC and resuspended in a 100mM $CaCl_2$ solution supplemented with glycerol at 10%. Cells were immediately frozen on a dry ice bath with ethanol and stored at -80ºC.

4.1.2 – DNA extraction (minilysats)

Transformed colonies were incubated in LB medium with 50µg/ml of Ampicillin or 2µl/ml of Chloranphenicol (see Table 3.2), ON at 37ºC. The culture was centrifugated for 2min at RT. Each pellet was ressuspended with 300µl of TS (50mM Tris pH 7,5 and 25% Sucrose) and mixed with 300µl of ELT (100mM EDTA, 2mg/ml Lysosyme and 0,1% TritonX100). The mixture was incubated 10min at RT and placed 10min at 70ºC before centrifugating for 15min at 4ºC. Pellets were discarded. Supernatants were then incubated with 550µl of 20% PEG6000, 1M NaCl for 30min at RT before centrifugation for 4min at high speed, to precipitate the plasmid. The pellets were then washed with 70% ethanol and ressuspended in TE 1x. Each minilysat was digested with the appropriate restriction enzyme and ran in an electroforese gel to confirm the identity of the plasmid amplified.

4.1.3 – DNA purification (phenol/chloroform method)

1 volume of phenol solution was added to the DNA in solution. After vortexing,

the mix was centrifugated for 1min to restore the two phases: Phenol (bottom phase), versus aqueous DNA solution, while contaminant proteins are left at the interphase (top phase). The DNA solution was then transferred to a new eppendorf tube, to which one volume of chloroform solution was added, forming two new phases. The mix was vortexed and centrifugated for 1min and the DNA solution was transferred to a new eppendorf tube. This step was repeated 3 times to remove any residual phenol. The purified DNA solution was then precipitated with three volumes of ethanol 100% supplemented with Ammonium Acetate to a final concentration of 2M. This mix was vortexed and centrifugated at 4ºC for 30min. The supernatant was discarded and the DNA pellet washed with 70% ethanol, was dried and ressuspended in TE 1x. The concentration of DNA was measured using the Nanodrop system.

4.2 – Cloning of the cDNA sequence used to generate a RNA specific probe for each actin gene.

4.2.1 – Transformation of competent cells with clone containing the cDNA for each actin gene

Clones containing the entire cDNA for each actin gene were ordered to the DGRC (see Table 3.2).

Table 3.2 – List of cDNA clones used to subclone for each actin gene. Each cDNA clone has a specific host vector and an antibiotic resistance gene.

Actin gene	cDNA clone	Host Vector	Antibiotic resistance
Actin 5C	GOLD RE 02927	pFLC-I	Ampicillin
Actin 42A	GOLD LD 18090	pBlueScript_SK(-)	Ampicillin
Actin 57B	EST LD 04994	pBlueScript_SK(-)	Ampicillin
Actin 79B	GOLD GH 04529	pOT2	Ampicillin
Actin 87E	EST AT 14584	pOTB7	Chloranphenicol

Each clone (conserved on a Waterman paper disc) was quickly washed with sterile TE 1x (1M Tris HCl pH 8,0 and 0,25M EDTA) and incubated on ice for 30min

with DH5α competent cells. Cells were heat shocked for 2min at 37ºC, transferred to 1ml of LB medium and incubated at 37ºC for 1h. Cells were then plated on LB supplemented with the appropriate antibiotic and incubated ON at 37ºC.

4.2.2 – PCR

In order to amplify the 3' UTR of each actin gene, 3' and 5' primers that flank the region of interest were designed. PCR primers generally range in length from 15-30 bases and should contain 40-60% of G + C (Promega Technical Guide). Primers designed for each actin gene are described in Table 3.3.

Table 3.3 – List of 5' and 3' primers used to amplify each actin 3'UTR sequences.

Gene	Primer	Sequence (5'→ 3')
Actin 5C	Act5C (3'UTR5')	GAAGGATCGCTTGTCTGG
	Act5C (3'UTR3')	GTAGTTCTTGTTATATTAAAGG
Actin 42A	Act42A (3'UTR5')	GCAGTAGTCGGGCTGGG
	Act42A (3'UTR3')	TTATTAAGAAGCGGTTACAAG
Actin 57B	Act57B (3'UTR5')	GCAGTTGCAGTTGCCTAG
	Act57B (3'UTR3')	CAATCATGAGATTATTTTACAT
Actin 79B	Act79B (3'UTR5')	GCATCCAAGCCACCCAAA
	Act79B (3'UTR3')	CACATGGGTTATTGGTTTTTA
Actin 87E	Act87E (3'UTR5')	GCGATCTAAACACCACAGA
	Act87E (3'UTR3')	AGATTTAATTTATAGAGGATGC

To perform the PCR, GoTaq buffer 5x, $MgCl_2$ solution 25mM, PCR nucleotide mix 10mM, upstream primer, downstream primer, GoTaq polymerase 5u/µl, DNA template and nuclease free water were mixed on ice. The PCR was performed in a thermal cycler with the following parameters: an initial 2min denaturating cycle at 95ºC, 35 cycles that included 1min of denaturation at 95ºC, 1min of annealing at 58ºC and 1min of extension at 72ºC, a final extension cycle of 5min at 72ºC and 1 cycle of soak at 4ºC for indefinite time.

4.2.3 – PCR product purification

Purification of each PCR product was performed using E.Z.N.A Gel Extraction Kit (Omega bio-tek). According to the kit instructions, the PCR product was separated by electrophoresis on an agarose gel. The DNA fragment of interest was excised using a UV light box. The gel slice weight was measured and binding buffer was added in a ratio of 10µl buffer: 10mg agarose gel slice. The mixture was incubated at 55-60ºC for 7min or until the gel was completely melted and centrifuged briefly at RT. The dissolved gel slice was applied to HiBind DNA spin-column and centrifugated for 1min at 14000rpm. Binding buffer was added to the column and centrifuged for 1min. The column was washed twice with the SPW buffer and centrifugated at RT for 1min. The column was centrifugated for 1min to dry the column matrix. Elution buffer was applied directly to the centre of the column to elute the DNA. The eluted DNA was kept at 4ºC or -20ºC.

4.2.4 – Ligation within the pGEM-T easy vector

The pGEM-T easy vector (Fig. 3.6) is a convenient system for cloning PCR products. The vectors are prepared by cutting with EcoRV and adding a 3' terminal thymidine to both ends. This, greatly improves the efficiency of the ligation of a PCR product into the plasmids by preventing recircularization of the vector and providing a compatible overhang for PCR products generated by certain thermostable polymerases (Promega technical manual).

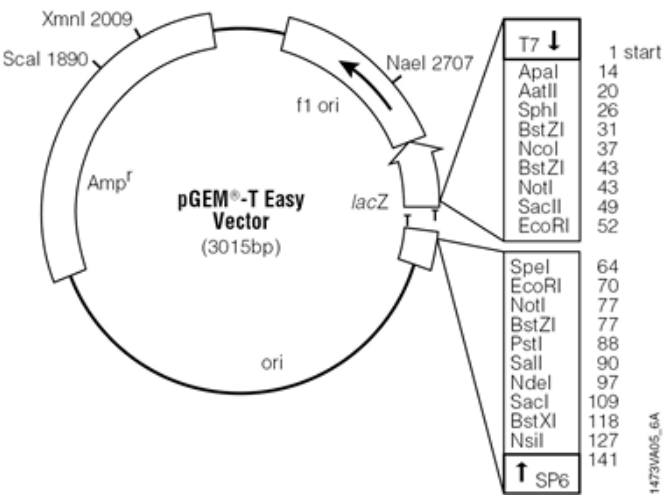

Figure 3.6 – Schematic representation of pGEM-T easy vector with restriction sites (adapted from Promega technical manual).

In order to ligate each PCR product corresponding to each actin isoforms 3'UTR sequence with the referred plasmid, purified PCR products were mixed with the vector in a 3 to 1 ratio, with 3 weiss/µl of T4 DNA ligase and 2x ligation buffer. The reaction was incubated for 1h at RT or ON at 4ºC.

4.2.5 – Transformation of competent cells with pGEM-T easy vector

One of the features of the pGEM-T easy vector (Promega) is the blue/white screening. The T7 and SP6 RNA polymerase promoters flank a multiple cloning region within the α- peptide coding region for β-galactosidase. Insertional inactivation of the α-peptide allows recombinant clones to be directly identified by colour screening on indicator plates (Promega technical manual). In order to amplify the DNA, the ligation reaction was mixed with DH5α competent cells and incubated on ice for 20min. Afterwards, a 90s incubation at 42ºC was done. The reaction was placed on ice for 2min. LB medium was added and incubated for 50min at 37ºC. XGal 20mg/ml and IPTG 0,8M were added to the LB Ampicillin (50µg/ml) plates. The culture was plated and incubated ON at 37ºC. The blue colonies (colonies with the insert) were picked and their DNA was extracted by minilysat method (described previously). To confirm the insertion, an

agarose gel electrophoresis was run. The resulted DNA solution will be used to perform specific probes.

5 – In situ *hybridization*

Since RNA probes are very sensitive to degradation by RNases, the water used for the whole *in situ* procedure was sterile and render RNase-free by a treatement with DEPC (Pyrokohlensauerdiethylester 97%, diethyl pyrocarbonate 97%).

5.1 – Probe synthesis

DNA templates were either linearized by digestion with the SpeI enzyme or with the SacII enzyme and then purified via phenol/chloroform extraction (see Section 4.1.3). The DNA template linearized with SpeI enzyme was transcribed with the T7 RNA polymerase to produce the sense probe and the DNA template linearized with SacII enzyme was transcribed with the Sp6 RNA polymerase to produce the anti-sense probe. The DIG RNA Labeling Kit (SP6/T7) (Roche) was used to produce the RNA probes labelled with digoxigenin-UTP. RNA labelling reaction was performed with 1µg of purified DNA template. To perform the transcription reaction, 10x NTP labelling mixture, 10x transcription buffer, protector RNase inhibitor, RNA polymerase SP6 or T7 and water were added to the DNA template, on ice. The reaction was incubated for 2h at 37ºC and centrifugated briefly. To confirm that transcription of each RNA probe was efficient, 1µl of each transcription sample was run on a 2% agarose gel. Each probe was then broken in pieces with a solution of 2x carbonate buffer at pH 10,2 (120mM Na_2CO_3 and 80mM $NaHCO_3$). The reaction was performed at 65ºC for 40min and stopped with a solution of 3M NaAc at pH 6,0. Each probe was then precipitated ON at -20ºC by adding 4M of LiCl, 20mg/ml of *E. coli* tRNA in 100% ethanol and centrifugated at 4ºC for 45min. The pellet was washed in 70% ethanol, centrifugated at 4ºC for 30min,

resuspended in water and stored at -20ºC.

5.2 – Fixation of imaginal discs

Flies used for the *in situ* hybridization experiment were *yw*. Third instar larvae wing imaginal discs were dissected in PBS and fixed in PBS, 4% FA, 67mM EGTA for 30min. Discs were washed several times in methanol. Afterwards, discs were washed with ethanol 100%.

5.3 – Hybridization

Discs were washed for 60min with a solution of 50:50 of xylene/ethanol in a glass vial and then rinsed several times with ethanol and at the end with methanol. Discs were fixed for 5min with a 50:50 solution of 5% FA in methanol/PBT and fixed for 30min with 5% FA in PBT. After washing with PBT, the discs were incubated for 8-10min in 20mg/ml proteinase K. Discs were washed with PBT. Afterwards, discs were fixed with 5% FA in PBT for 30min at RT or ON at 4ºC and washed 10min with a solution of 50:50 of PBT/hybridization solution. Hybridization (hyb) solution is 50% formamide, 5x standard saline citrate (SSC), 100µg/ml heparin, 0,1% Tween 20 and 100µg/ml boiled salmon sperm DNA (ssDNA). Discs were incubated for 3hs in hyb solution at 55ºC. Discs were hybridized in 2µl of probe diluted in 60µl of hyb solution for 18-20hs at 55ºC. Rinsed with hyb solution and incubated in the same solution for 3hs at 55ºC.

5.4 – Pre-absortion of anti-digoxigenin (anti-DIG) antibody

yw embryos were collected after an ON collection, washed with water and bleached for 5min. Then, the embryos were washed thoroughly. Embryos were fixed in a solution of 1:1 of PBS and heptane with 4% FA for 30min and washed in a 1:1 solution of methanol and heptane. Then, embryos were washed 3 times with methanol and 3 times with PBT. Embryos were blocked in a PBT 1% BSA for 1h. The volume of embryos was

estimated. For 1 volume of embryos, a volume of anti-DIG antibody (Jackson ImmunoResearch) and 4 volumes of PBT were added. Embryos were incubated ON at 4ºC with shacking and centrifuged 5min at 4ºC. 1µl of azide 10% was added to 500µl of supernatant.

5.5 – Anti-DIG alkaline phosphatase reaction – Staining Reaction

Discs were successively washed at RT with decreasing series of hyb solution: 75% hyb in PBT, 50% hyb in PBT, 25% hyb in PBT and with PBT for 1h. Discs were incubated with the anti-DIG antibody, previously pre-absorbed ON at 4ºC at a 1:2000 final dilution. The following day, discs were washed several times for 1h in PBT before a final wash with the staining buffer (0,1M NaCl, 0,05M $MgCl_2$, 0,1M Tris-HCl pH9,5 and 0,1% Tween 20). Revelation was performed in the dark with 20µl of NBT/BCIP solution (Roche) in the staining solution. To follow the staining reaction, discs were observed under a microscope from time to time. The reaction was stopped by 2 washes with the staining buffer and then rinsed with PBT and several times with ethanol 100%. Discs were then rehydrated in ethanol series in PBT and mounted in glycerol 80%.

IV – Results

It was shown by Janody and Treisman that mutant cells for CP induce excessive actin filaments polymerization. In this study, I want to investigate if the phenotype observed when the CP is lost is a consequence of excessive actin filaments accumulation. To do so, I used an overexpression approach, instead of a loss of function, to get more insights on whether each *Drosophila* actin genes have specific functions. In order to determine whether the overexpression of any specific actin isoform gives a similar phenotype to the loss of CP, which is the extrusion and death of wing blade cells, I analysed the developmental consequences of overexpressing each of the six actin genes during epithelial morphogenesis. To achieve this goal, I generated recombinant *Drosophila* lines, between transgenes that encode for either of the six actin genes fused to green fluorescent protein (GFP) and placed under the control of UAS-sites and FRT-sites. Afterwards, I expressed either of the six *actin-GFP* genes using the UAS-Gal4 (Brand and Perrimon, 1993) and the Gal80 (Lee and Luo, 2001) systems to drive expression in wing imaginal discs.

1 – All fly actin genes are overexpressed at a comparable level.

Each actin cDNA fused to GFP was inserted into the *Drosophila* genome randomly by P-element transformation. Due to site specific chromatin organization, the accessibility to the UAS-sites, upstream of each *actin-GFP* target gene, can vary from one transgenic line to another, leading to different expression levels between each one. Since I want to determine whether any of the six actin isoforms, when overexpressed, gives similar phenotypes to the loss of *CP* and compare the behaviour of cells overexpressing specific actin genes, it is crucial to determine the expression level of each

Actin-GFP fusion protein.

To do so, I crossed females carrying the *daugtherless*-Gal4 (*da*-Gal4) driver to males bearing either one of the *actin-GFP* constructs. The *da*-Gal4 driver will express each target gene ubiquitously in the ectoderm. Embryos resulting from these crosses were collected to produce protein extracts that were analysed by Western Blot (see Materials and Methods). The membrane was blotted with an anti-GFP antibody that revealed a band of around 70KDa in each extract, while control $y^{-}w^{-}$ embryonic extracts showed no signal (Fig. 4.1). The intensity of the GFP signal for each Actin-GFP isoform, although showed small variations between each other, these variations did not appear to be significant (Fig. 4.1A).

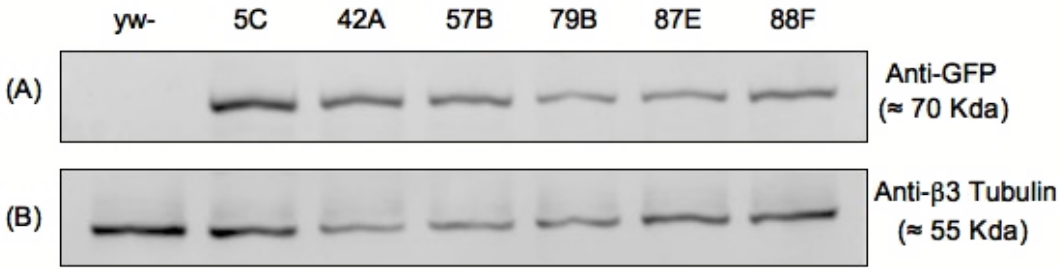

Figure 4.1 – Western blot from *Drosophila* embryonic extracts, expressing each of the six *Drosophila* actin genes fused to GFP under the control of *da*-Gal4 driver. The first lane indicates *Drosophila* embryonic extracts from *y-w-* embryos that do not express GFP. (A) Blot marked with the anti-GFP antibody that reveals each of the Actin-GFP fusion proteins. (B) Same blot marked with the Anti-β3 Tubulin antibody used as a reference to evaluate the quantity of loading extracts.

the signal given with the anti-β3 Tubulin antibody and the anti-GFP antibody for each genotype allowed me to compare the expression level for each Actin-GFP fusion protein (Chart 4.1).

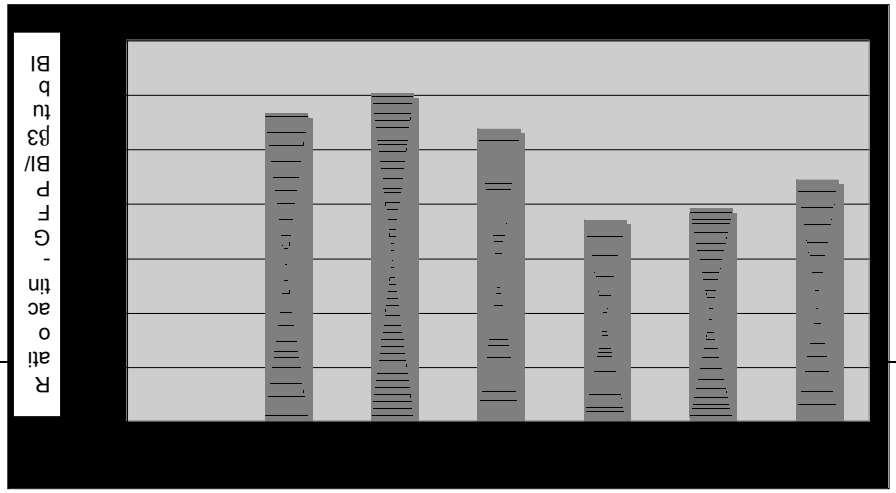

Chart 4.1 – Graph showing the ratio between the intensity of the signal obtained with the anti-β3 Tubulin antibody and the anti-GFP antibody for each genotype. Blue indicates cytoplasmic actins, yellow indicates larval muscle actins and pink indicates adult muscle actins.

Chart 4.1 also indicates that the intensity of the GFP staining for each Actin-GFP fusion protein has some variations and despite the fact that the major variation observed in Chart 4.1 is 0,74 fold, between the Actin 42A-GFP and Actin 79B-GFP overexpression, I assumed that those variations were not significant.

Therefore, the consequences of overexpressing each of the *actin-GFP* genes in disc epithelial tissues can be compared regardless of the different expression levels.

2 – Actin isoforms incorporate in filaments at various subcellular locations within the wing disc when overexpressed.

The six *Drosophila* actin isoforms, when ectopically expressed, have the ability to associate with certain structures formed by endogenous actins, such as filopodia/lamellipodia, cortical actin, basal stress fibers, ring canals, actin struts, larval/adult muscles and Z-lines (Röper *et al.*, 2005). Although the difference in the efficiency of incorporation into these structures is small, the different actin isoforms behave far from identically (Röper *et al*., 2005). In order to determine whether each actin-GFP isoform, when overexpressed in the wing imaginal disc, incorporates within actin filaments in specific subcellular locations, I overexpressed each of the 6 actin genes fused to GFP, by using the *engrailed*-Gal4 (*en*-Gal4) driver. Since *en*-Gal4 drives the

expression of the UAS-target gene in the posterior compartment of the wing discs during all stages of larval development (Fig. 4.4 A), the anterior compartment can be used as a wild type control. Discs were stained with Phalloidin to reveal actin filaments (Fig. 4.2 A'-L'), and GFP revealed expression of each actin-GFP isoform in the posterior compartment (Fig. 4.2 A-L).

As expected, overexpressing either of the 6 actin-GFP isoforms promote excessive actin filaments formation in the posterior compartment of the wing imaginal disc (Fig. 4.2). Interestingly, actin filaments were observed to accumulate in different locations within the cell, depending of the Actin-GFP isoform overexpressed. For instance, Actin 5C-GFP (Fig. 4.2 G') and Actin 57B-GFP (Fig. 4.2 I') were mostly incorporated in filaments formed at the basal surface of wing disc epithelium. In contrast, Actin 42A-GFP (Fig. 4.2 B'), 79B-GFP (Fig. 4.2 D'), 87E-GFP (Fig. 4.2 E') and 88F-GFP (Fig. 4.2 F') were mostly incorporated in actin filaments at the apical surface of the wing disc epithelium. Further analysis of the F1 progeny of this set of experiment will be analysed in following sections.

This data shows that in the wing imaginal discs, each actin isoform, when overexpressed, might get incorporated in specific actin filaments structures within the cells. All together, this suggests that while the actin isoforms have very similar sequences, differing in only a few aminoacid residues, each one have specific cellular properties.

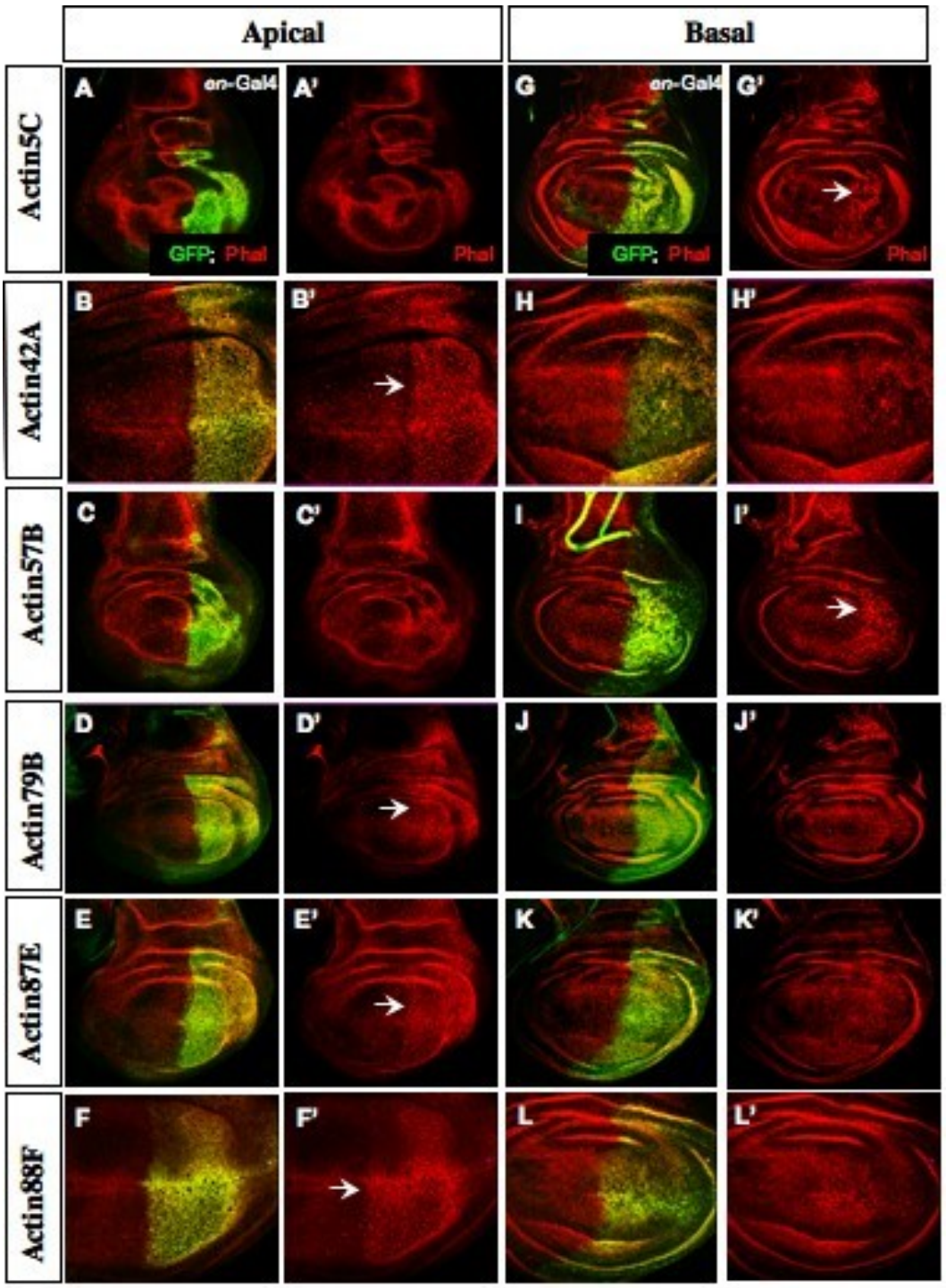

Figure 4.2 – Incorporation of the different actin isoforms in filaments in various locations of the wing disc. All panels show standard confocal sections of third instar wing imaginal discs marked with GFP in green, which reveals each of the Actin-GFP fusion protein, and Phalloidin in red, which reveals F-actin. (A-F') Apical sections. (G-L') Basal sections. (A-L) Merged. (A'-L') Phalloidin staining alone. The white arrows in G', B', I', D', E', and F' indicate strong actin filaments staining in the posterior compartment. Overexpression of Actin 42A-GFP, 79B-GFP, 87E-GFP and 88F-GFP in the *en*-expression domain were mostly incorporated in filaments at apical sites, while actin 5C-GFP and 57B-GFP were mostly incorporated in filaments at basal sites.

3 – Although each of the actin-GFP genes is expressed at similar levels, their overexpression in the wing imaginal disc give rise to damaged adult wings of different strength.

Since overexpression of either of the six actin isoforms lead to their incorporation in actin filaments at different locations within the cell, I investigated whether this behaviour could lead to different adult developmental consequences when the overexpression is driven mainly in the wing blade region. To do so, I overexpressed either of the 6 actin genes fused to GFP, by using the *nubbin*-Gal4 (*nb*-Gal4) driver. The flies were grown at 27,5ºC (see Materials and Methods).

The adult flies that overexpressed Actin 5C, 42A and 57B, displayed severely damaged wings (Fig. 4.3 B-D'), while flies overexpressing Actin 79B, 87E and 88F had less damaged wings (Fig. 4.3 E'-G'). Moreover, the wing size of those that overexpressed Actin 5C, 42A and 57B was severely reduced and also showed blisters, notches, necrotic spots and mispatterned veins and bristles (Fig. 4.3 B'-D').

In particular, the overexpression of Actin 57B gave the stronger wing defects, while overexpression of Actin 87E gave the weakest defects observed. In addition, overexpression of Actin 5C and 57B gave several necrotic spots in the wing proper. Moreover, the overexpression of Actin 42A gave a specific defect, not observed in the overexpression of the other actin isoforms, namely blistering formation. In addition, the defects observed in the adult wing for Actin 57B overexpression are more sever when compared to the defects observed in the adult wing for Actin 42A overexpression, although in Chart 4.1 the level of overexpression of Actin 57B is slightly lower than Actin 42A. This suggests that the phenotypes observed for each actin isoform overexpression might be specific of each actin gene, instead of a difference on the level of overexpression.

Weaker defects were observed in fly wings, when the other actin isoforms (79B, 87E and 88F) were overexpressed. These phenotypes were mainly notches and veins bifurcation. Together this set of experiments show that each actin-GFP gene when

overexpressed in the wing, can lead to distinct defects and differential strength of defects in the wings, although all actin genes are expressed at similar levels.

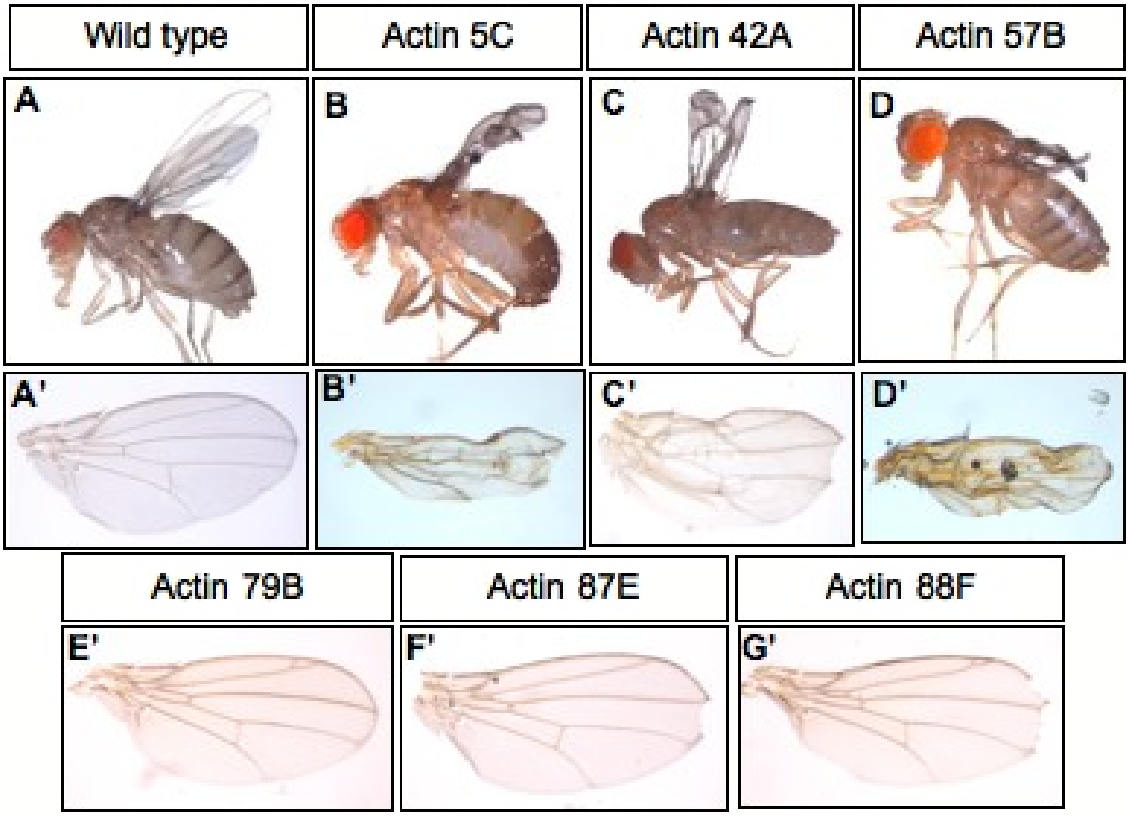

Figure 4.3 – Overexpression of either of the six actin genes in *nb* expression domain lead to several wing defects at 27,5ºC. (A-A') Wild type adult fly and wild type adult wing, respectively. (B-G) Adult flies showing damaged wings. (B'-G') Adult wings showing development defects. Overexpression of actin 5C, 42A and 57B genes with *nb* driver lead to several deleterious consequences in adult wings, like blistering, notches, necrotic spots and mispatterned veins and bristles, while actin 79B, 87E and 88F lead to weaker defects, like notches and vein

4 – Overexpression of each of the six actin genes gives specific developmental phenotype that are time and cell-type dependent.

In order to gain some insights of the cellular consequences of the overexpression of the actin isoforms that could explain the adult phenotypes previously described, I overexpressed each of the six actin-GFP genes in different regions of the wing imaginal disc epithelium at different time of the larval development. To do that, I used different drivers such as *en*-Gal4, *sd*-Gal4 and *nb*-Gal4. These drivers drive the expression of the UAS-target genes at different developmental stages and in different regions within the wing disc. The *en*-Gal4 drives the expression of target genes at embryonic stages in the posterior compartment and also during larval development (Fig. 4.4 A). The *sd*-Gal4 drives the expression of target genes at early stages (1st instar larvae) more broadly in the whole wing epithelium and as development proceeds its expression gets restricted to the wing blade and hinge (Fig. 4.4 B). Finally, *nb*-Gal4 drives the expression of target genes, at 2nd instar larvae, in the wing blade and first ring of the wing hinge (Fig. 4.4 C).

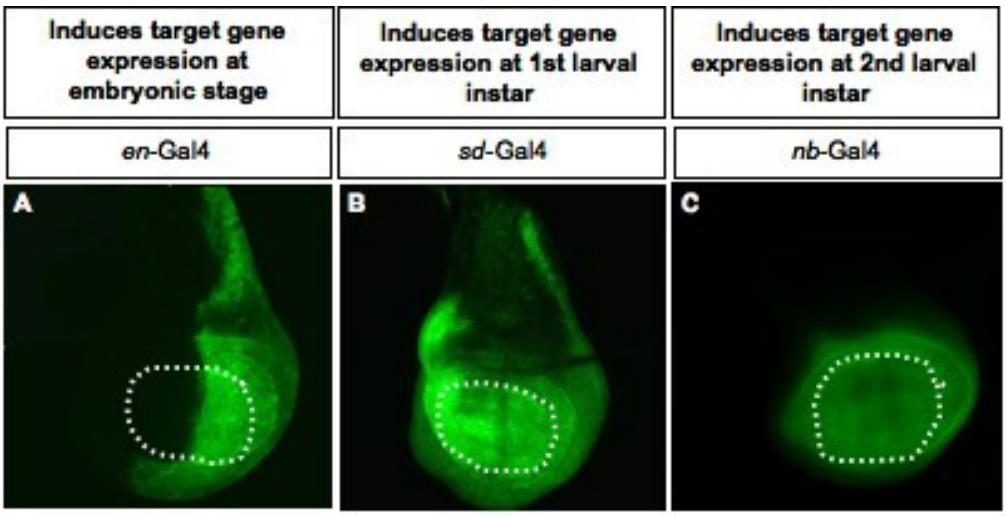

Fig. 4.4 – Domain of expression of UAS-CD8GFP targeted by Gal4 drivers expressed in third instar larvae wing imaginal disc. All panels show standard confocal sections of third instar wing imaginal discs marked with CD8-GFP in green and with the wing blade delimited by dashed lines. (A) *engrailed*-Gal4 driver expression domain. (B) *scalloped*-Gal4 driver expression domain. (C) *nubbin*-Gal4 driver expression domain.

Table 4.1 summarizes the developmental consequences scored by the overexpression of each *actin-GFP* gene in the wing discs using 3 independent Gal4 drivers (*nb*-Gal4; *en*-Gal4; *sd*-Gal4) and also the phenotypes observed after the induction of clones overexpressing the actin genes. Each colour highlight the identical phenotypes observed following overexpression of different *actin-GFP* genes, suggesting that these actin isoforms might be involved in similar developmental process. While in principle, all Actin-GFP genes are overexpressed at similar levels (Fig. 4.1), not all induce identical cellular phenotypes. The different outcomes scored seem to be dependent on the developmental stage (1st instar or 2nd instar larvae) at which each actin-GFP is overexpressed and on the tissue overexpressing each actin-GFP. In the following sections I will carefully describe and analyse each of the cellular behaviours shown in Table 4.1.

Table 4.1 – Summary of the divers developmental consequences observed following the overexpression of each actin-GFP gene in wing discs by using several Gal4 drivers and in clones of cells. The consequences of overexpressing each *actin gene* (X axis) where classified based on the phenotype observed (Y2 axis) in different regions of the wing imaginal disc (Y1 axis) by using different overexpression conditions (Y3 axis). (+) means that the phenotype was observed. (-) means that the phenotype was not observed. (+/-) means that the phenotype was weak or not reproducible from one disc to another. Blue indicates hinge overgrowth; Red indicates a possible cell competition mechanism; Orange indicates smaller wing blade than wild type; Yellow indicates cell migration and; Green indicates survival of cells after extrusion. Boxes in black mean that the experiment was not determined.

			Act5C Act5C	Act42A Act42A	Act57B Act57B	Act79B Act79B	Act87E Act87E	Act88F Act88F
		en-Gal4	+	+	+	-	-	-
Hinge	Overgrowth	ab-Gal4	+	+	+			
Hinge	Overgrowth	ad-Gal4	+	+	+			
		ed-Gal4	+	+	+	+/-	+/-	+/-
Hinge	Cell death	ab-Gal4	+	+	+			
Hinge	Cell death	ad-Gal4	+	+	+			
	Cell death	eb-Gal4 clones	+/-	+/-	+/-	-	+/-	+/-
	Wg upregulation	eb-Gal4 clones	+/-	+/-	+/-	-	+/-	+/-
	Wg upregulation	en-Gal4	+	+	+	+	+/-	+
Blade	Cell death	ab-Gal4	+	+	+			
Blade	Cell death	ad-Gal4	±	±	±			
	Cell death	ed-Gal4 clones	±	±	±	±	±	±
		eb-Gal4 clones	+	+	+	+	-	+
Blade	Small wing blade	ab-Gal4	+	+	+			
Blade	Small wing blade	ad-Gal4	+	-	+			
Blade		ed-Gal4	+	-	+	=	+	+
Blade	Cell migration	ab-Gal4	+	+	+		+	+
Blade	Cell migration	ad-Gal4			+			
Blade	Size	eb-Gal4 clones						
Blade	Cell still maintained	clones	+/-	<<	±	±	±	+/-
Blade	Cell extrusion maintained	eb-Gal4 clones	+/-	+/-	+			
Blade	Cell extrusion survive	nb-Gal4	+	+	+			
	Cell still survive	nb-Gal4	+	+	+			

4.1 – Only Actin 5C, 42A and 57B promote hinge overgrowth, associated to ectopic wingless expression, when overexpressed.

4.1.1 – Overexpression of Actin 5C, 42A and 57B promote hinge overgrowth.

In order to compare, at the cellular level, the consequences of overexpressing each of the six *actin-GFP* isoforms, I analysed, in the *engrailed* set of experiments some cellular markers. In these experiments, the anterior compartment serves as control (Fig. 4.4 A). I crossed females carrying the *en*-Gal4 driver to males bearing either one of the *actin-GFP* constructs. Wing discs from the F1 progeny were stained with the anti-Armadillo antibody to outline the cell membrane, and with anti-activated-Caspase 3 antibody that reveals Caspase-dependent cell death.

Interestingly, overexpression of the two cytoplasmic actins (*actin 5C-GFP* and *42A-GFP*) (arrow in Fig. 4.5 A'-B') and the larval muscle actin *57B-GFP* (arrow in Fig. 4.5 C') induce wing hinge expansion in the *en*-expression domain, while overexpression of the 3 remaining *actin-GFP* genes does not have such effect (Fig. 4.5 D'-F'). Hinge sizes were compared, based on Armadillo staining, between the posterior actin-GFP-expressing compartment and the anterior wild type compartment by measuring the distance between hinge foldings (See Material and Methods). While the hinge measurement in the posterior compartment was bigger for *actin 5C-GFP, 42A-GFP* and *57B-GFP* experiments (Fig. 4.5 A'-C'), compared to the anterior compartment, no measurement difference could be observed for *actin 79B-GFP*, *88F-GFP* and *87E-GFP* overexpression (Fig. 4.5 D'-F').

To follow these observations, I overexpressed the six actin-GFP fusion genes with the *scalloped*-Gal4 (*sd*-Gal4) driver, first ubiquitously expressed in the whole wing and then restricted the wing blade and hinge at later larval stages (Fig. 4.4 B). A similar hinge overgrowth phenotype to the previous set of experiments was observed in the wing disc for *actin 5C-GFP, 42A-GFP* and *57B-GFP* overexpression (Appendix I, Fig. I.1 A'-C'). However, hinge overgrowths were not observed in the case of the three remaining *actins-*

GFP fusion genes (Appendix I, Fig. I.1 D'-F').

As expected, when *actin 5C-GFP, 42A-GFP* and *57B-GFP* were overexpressed in the *nubbin*-Gal4 (*nb*-Gal4) expression domain, similar overgrowths were scored in the hinge (Appendix I, Fig. I.2 A'-C'). In this case, the *nb*-Gal4 driver drives expression of target genes from 2nd instar larvae stages onwards, in a domain that comprises the wing blade and only the first ring of the hinge. Thus, in the hinge epithelium, two independent groups of actin genes seem to behave in different ways when overexpressed. The *actin 5C, 42A* and *57B* seem to promote growth, while *actin 79B, 88F* and *87E* do not appear to have any effect on all growth in the hinge. Moreover this implies that for *actin 5C*, *42A* and *57B* endogenous expression has to be tightly regulated to restrict growth. Since the hinge overgrowth was observed using either of the Gal4 drivers (*en*, *sd* and *nb*-Gal4) and each of them start to be express at different developmental stages, this set of experiments also suggests that the overproliferation may not be time-dependent.

Moreover, the hinge overgrowth observed with the three drivers for *actin 5C, 42A* and *57B* appears to be associated to large number cell death seen by activated-Caspase 3-positive cells in the hinge (Fig. 4.5 A''-C''; Appendix I, Fig. I.1 A''-C''; Appendix I, Fig. I.2 A''-C''). However, the overexpression of *actin 79B, 87E*, and *88F* seems to induce fewer or no cell death in the hinge (Fig. 4.5 D''-F''; Appendix I, Fig. I.1 D''-F''). All together, this data shows that while hinge cells overexpressing *actin 5C, 42A* and *57B* lose proliferation control, some of them fail to survive and undergo apoptosis.

Overexpression of most of the actin genes also seems to affect cell survival in the wing blade epithelium (Fig. 4.5 A''-F''; Appendix I, Fig. I.1 A''-F''; Appendix I, Fig. I.2 A''-C''). This issue will be further discussed in Section 4.2.

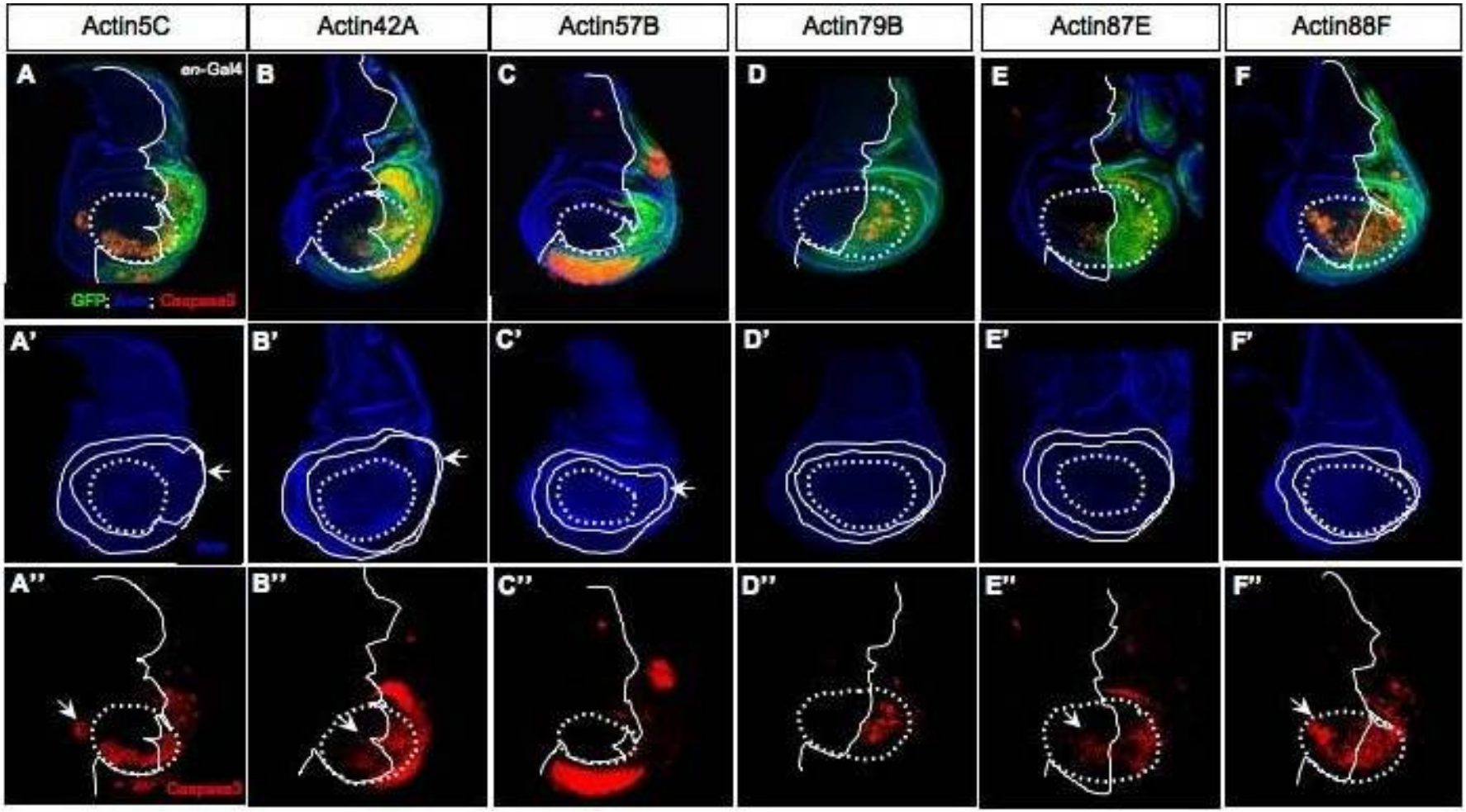

Fig. 4.5 – Overexpression of *actin 5C-GFP, 42A-GFP* and *57B-GFP*, with the *en*-Gal4 driver, promote hinge expansion. All panels show standard confocal sections of third instar wing imaginal discs marked with GFP in green, which reveals each of the Actin-GFP fusion protein, Armadillo in blue, outlines the apical cell membrane, and activated-Caspase3 in red marks Caspase-dependant cell death. (A-F) Merged. (A'-F') Armadillo channel with wing blade delimitaded with punctuated line and hinge delimited with plain lines. (A''-F'') Activated-Caspase 3 channel with wing blade delimited with punctuated line. The white arrows in A', B' and C' indicate hinge overgrowth when actin-GFP is overexpressed. The white arrows in A'', B'', E'' and F'' indicate cells overexpressing actin that are recovered far away from where they originate. (A''-F'') Overexpression of all actin genes leads to death in blade and hinge of wing disc.

4.1.2 – Hinge overgrowth is associated to Wg upregulation.

Since overexpression of *actin 5C, 42A* and *57B* leads to hinge overgrowth I wondered whether such overgrowth would be related to Wingless (Wg) upregulation. To do so, I analysed Wg upregulation in wing discs overexpressing either of the 6 actin genes in the *en*-expression domain. Wg is a major developmental regulator of epithelial tissue growth in flies, which seems to be upregulated in some situation where growth control is affected (Saucedo and Edgar, 2007). The secreted signaling molecule encoded by *wg* is expressed in two concentric rings in the wing hinge in addition to the wing blade. Moreover, there are evidences that suggest that *wg* is principally required for local cell proliferation in the hinge. For instance, loss of *wg* expression leads to a local reduction in cell division, resulting in the deletion of a distinct set of wing hinge structures. Conversely, overexpression of *wg* or activation of the *wg* pathway leads to hinge overgrowth (Neumann and Cohen, 1996). Interestingly, loss of either subunit of the *capping protein* $\alpha\beta$ heterodimer *(CP)*, which induces excessive actin polymerization, promotes hinge overgrowth associated to Wg upregulation (Janody and Treisman, 2006). Not surprisingly, I found that Wg was upregulated in the posterior hinge compartment, when *actin 5C, 42A and 57B* were overexpressed (arrow in Fig. 4.6 A'-C') but, interestingly it was not disrupted following the overexpression of *actin 79B, 87E* and *88F* (Fig. 4.6 D'-F'). This suggests that hinge overgrowth induced by *actin 5C, 42A* and *57B* overexpression is a consequence of Wg upregulation. All together, this set of data suggests that CP might prevent polymerization of actin 5C, 42A and 57B to restrict Wg expression and growth in the hinge.

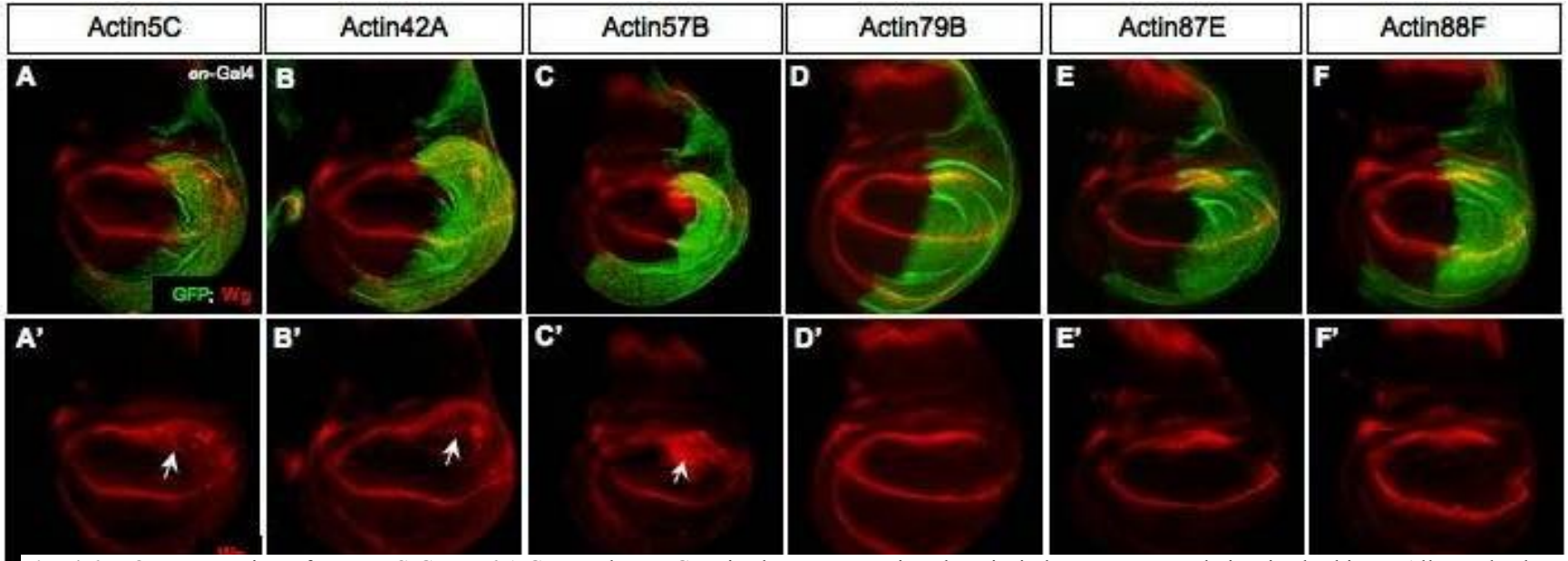

Fig. 4.6 – Overexpression of *actin 5C-GFP, 42A-GFP* and *57B-GFP* in the *en*-expression domain induce Wg upregulation in the hinge. All panels show standard confocal sections of third instar wing imaginal discs marked with GFP in green, which reveals each of the Actin-GFP fusion protein and Wingless in red. (A-F) Merged. (A'-F') Wingless expression. The white arrows in A', B' and C' indicate the upregulation of Wg in the hinge.

red. (A-F) Merged. (A'-F') Wingless expression. The white arrows in A', B' and C' indicate the upregulation of Wg in the hinge.

4.2 – *actin 5C* and *57B,* when overexpressed at early stages, prevent wing blade growth.

Interestingly, driving overexpression of *actin 5C-GFP* and *57B-GFP* using the *sd*-Gal4 driver resulted in a reduced size wing blade accompanied by hinge overgrowth (Fig. 4.7 A-B') when compared to a wild type situation (Fig. 4.4 B). However, the wing blade of discs overexpression *actin 5C-GFP* and *57B-GFP* using the *nb*-Gal4 driver do not result in major wing blade size defects (Fig. 4.7 E-F'). This differential behaviour could be due to a dosage effect since the *sd*-Gal4 and *nb*-Gal4 drivers are unlikely to induce gene expression at identical levels. For instance, *sd*-Gal4 might be a strong activator, inducing robust overexpression of *actin 5C-GFP* and *57B-GFP*, which would be very deleterious for wing blade growth, while *nb*-Gal4 might be a weak activator. Alternatively, these differences could be due to different developmental stages in which each driver is expressed. The *sd*-Gal4 driver induces expression of target genes at 1st instar larvae (Campbell et al., 1992), while the *nb*-Gal4 driver promotes target gene expression at 2nd instar larvae (Anderson et al., 1995). Therefore, the overexpression of *actin 5C* and *57B* might prevent growth of the wing blade only at early larval stages, while has no effect on cell growth at later stages. In support of the time-dependent effect, overexpression of *actin 5C-GFP* and *57B-GFP* with *en*-Gal4, which is expressed from embryogenesis to adulthood (Kassis, 1990), also resulted in reduced wing blade size in the posterior compartment (Fig. 4.7 C-D'). In addition, *sd*-Gal4 and *nb*-Gal4, both promote hinge overgrowth, when driving the overexpression of *actin 5C-GFP* and *57B-GFP*. Finally, since this phenotype was not observed when the other *actin-GFP* genes were overexpressed (see Section 4.1.1), the growth phenotype induced by *actin 5C-GFP* and *57B-GFP* overexpression might be the consequence of specific properties of each of these actin isoforms when overexpressed.

I also noticed that, when overexpression of actin 5C and 57B is driven by the *nb*-Gal4 driver, there appeared a lot of cell death in the blade region, seen by activated-Caspase 3-positive cells (Fig. 4.7 E''-F''). In contrast, using *sd*-Gal4, no cell death could be observed in the blade (Fig. 4.7 A''-B''), suggesting that at early stages the wing blade

cells may be more resistant to cell death than at later stages.

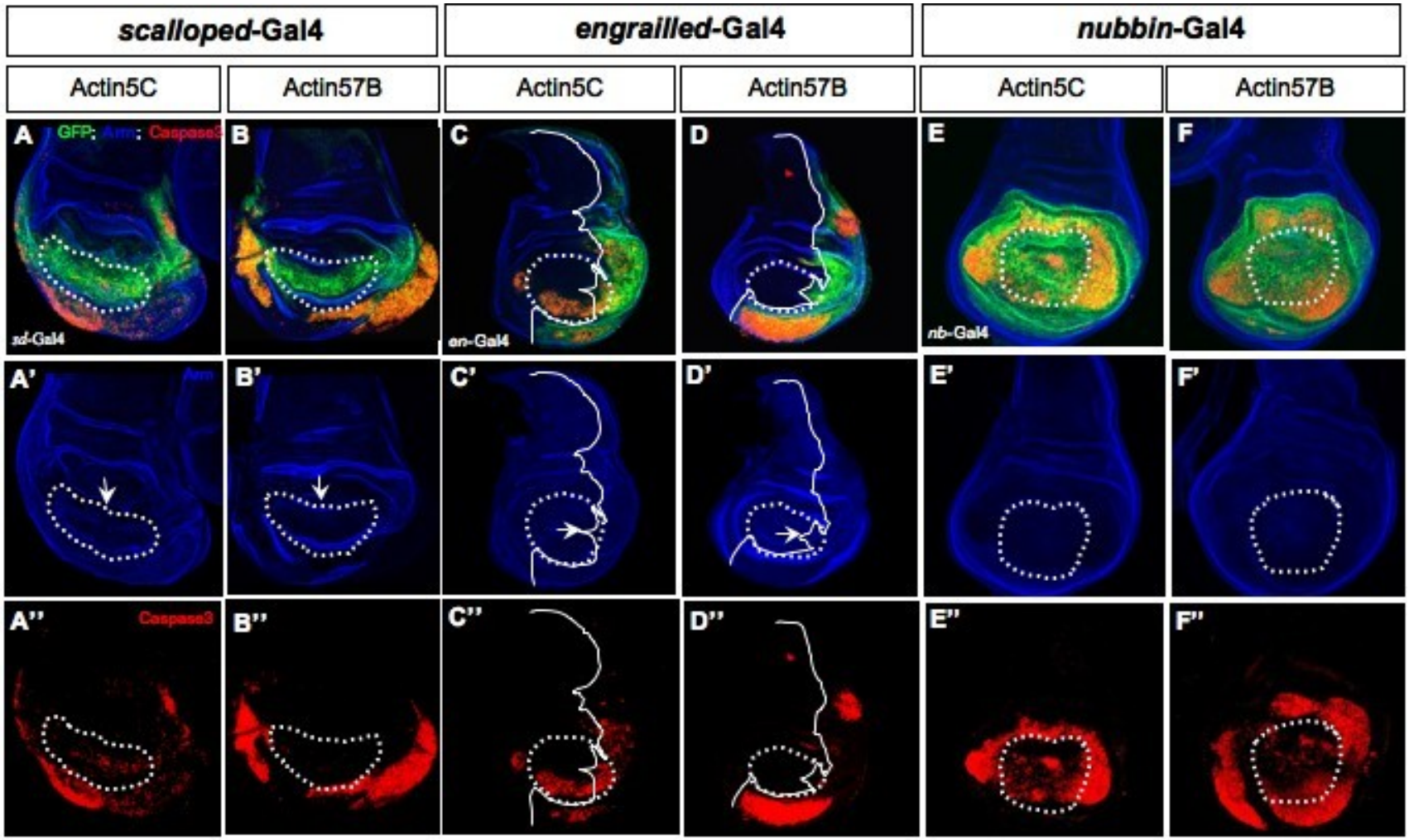

Fig. 4.7 – Overexpression of *actin 5C-GFP* and *57B-GFP* prevent growth of wing blade cells only at early larval stage. All panels show standard confocal sections of third instar wing imaginal discs marked with GFP in green, which reveals each of the Actin-GFP fusion proteins, Armadillo in blue outlines the apical cell membrane, and activated-Caspase3 in red marks Caspase-dependant cell death. (A-F) Merged with wing hinge delimited with punctuated line. (A'-F') Armadillo alone with wing blade delimited with punctuated line. (A''-F'') Activated-Caspase 3 alone with wing blade delimited with punctuated line. (A-B') Overexpression of *actin 5C-GFP* and *57B-GFP* in the *sd*-expression domain. (C-D') Overexpression of *actin 5C-GFP* and *57B-GFP* in the *en*-expression domain. (E-F') Overexpression of *actin 5C-GFP* and *57B-GFP* in the *nb*-expression domain. The white arrows indicate reduced wing blades.

4.3 – The cellular environment might influence the behaviour of *actin*-overexpressing cells.

4.3.1 – Cells apposed to each other, expressing different levels of *actin 42A*, influence each other behaviour.

Interestingly, very few *actin 42A-GFP*-overexpressing cells could be recovered in the wing blade when driven with the *en*-Gal4 driver, expressed only in the posterior compartment of the wing imaginal disc (Fig. 4.8 A, compare the reduced number of GFP-positive cells in the wing blade). However, overexpression of *actin 42A* using the *sd*-Gal4 driver does not affect wing blade cell death but instead, seems to promote an increase in wing blade size (Fig. 4.8 B). Moreover, when I induce groups of cells overexpressing *actin 42A*, surrounded by wild type cells, by using the MARCM system, the cells that overexpress Actin 42A extrude from the epithelium and die by apoptosis (Fig. 4.9 B-B'). This suggests that *actin 42A*-overexpressing cells, when apposed to wild type cells, are eliminated by a process of cell competition. Cell competition is a type of short-range-interaction between cells expressing different levels of a particular protein, in which the "loser" cells disappear from the tissue, whereas the "winner" cells survive and proliferate (reviewed in Moreno, 2008). Therefore, in the blade region, the interface between posterior *en*-Gal4>*actin 42A-GFP*-overexpressing cells and anterior wild-type cells seems to promote non-autonomous death of posterior *en*-Gal4>*actin 42A-GFP*-overexpressing cells (Fig. 4.8 A). In a similar manner, *actin 42A*-overexpressing cells in clones die in the blade region, probably due to differences in expression level between *actin 42A*-overexpressing cells and surrounding wild-type cells (Fig. 4.9 B). In this context, *actin 42A*-overexpressing cells would be the looser cells, while wild type apposed cells would be the winner cells. However, when the whole tissue overexpresses *actin 42A*, these cells instead seem to overproliferate (Fig. 4.8B). All together this data suggests, that the behaviour of cells overexpressing *actin 42A* depends on the cellular environment.

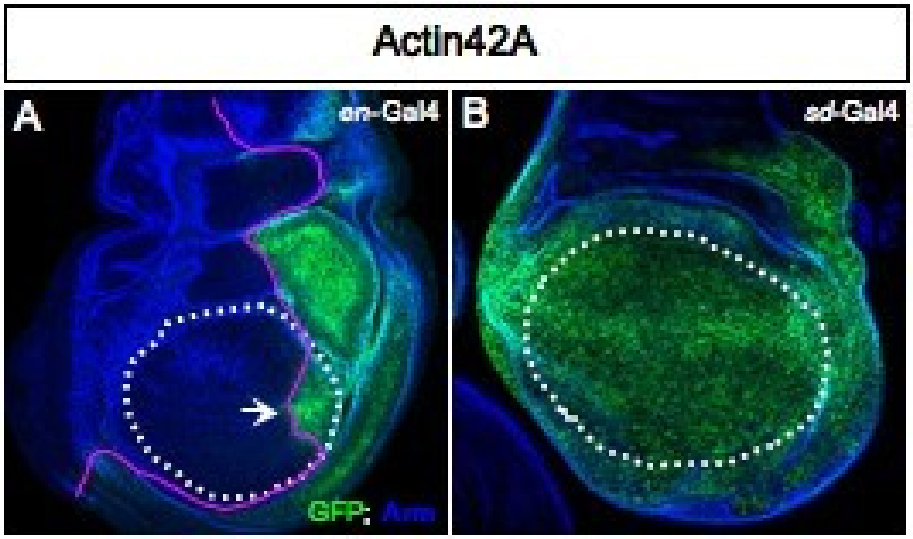

Fig. 4.8 – Overexpression of *actin 42A-GFP* leads to different behaviour depending on the surrounding environment. The panels show standard confocal sections of third instar wing imaginal discs marked with GFP in green, which reveals 42A Actin-GFP fusion protein, and anti-Armadillo antibody in blue, which outline the apical cell membrane. (A) *actin 42A-GFP* overexpression in the *en*-expression domain. (B) *actin 42A-GFP* overexpression in the *sd*-expression domain. The wing blade is delimited by a white punctuated line. *actin 42A-GFP* overexpression with the *en*-Gal4 driver leads to a small posterior wing blade while with the *sd*-Gal4 driver promotes blade proliferation.

4.3.2 – Groups of cells overexpressing actin genes give specific developmental phenotypes that are cell-type dependent.

In order to analyse the developmental consequences of overexpressing each of the six actin-GFP genes in different regions of the wing imaginal disc epithelium, I analysed the behaviour of a small subset of overexpressing-cells in a wild-type tissue. To do this, I overexpressed each of the six actin genes using the MARCM system (described in Chapter 1; Lee and Luo, 1999). Clones marked positively by GFP, overexpressing either of the six *actin-GFP* isoforms, were induced at first and second larval instar and stained with an anti-Armadillo antibody, to outline the apical cell membrane, and an anti-activated Caspase 3 antibody, to reveal Caspase-dependent death cells.

Fig. 4.9 A-F shows that groups of cells overexpressing each *actin-GFP* gene could be recovered in all regions of the wing disc epithelium. A large number of clones

were activated-Caspase 3 positives, suggesting that those cells were eliminated by apoptosis (Fig. 4.9 A-F). Optical cross-sections through the wing disc epithelium showed that actin-overexpressing cells lost their polarity and were found on the basal surface of the wing disc. Interestingly, some cells could still be maintained within the epithelium, such as the clones overexpressing actin 79B (Fig. 4.9 D'). Caspase3-positive cells were observed when either of the actin-GFP genes were overexpressed in clones, but this apoptotic phenotype was observed mostly in specific regions of the wing disc: the blade and hinge. For instance, clones of cells overexpressing actin 5C, 42A and 57B promote cell death more in the blade, but still, some in the hinge. Clones of cells overexpressing actin 79B and 88F promote death only in the wing blade, while in clones of cells overexpressing actin 87E cell death was only observed the hinge region. It is important to mention that, these overexpression experiments in clones might have a mixture of phenotypes with different underlying cellular mechanisms occurring at the same time. This is due to the fact that the overexpression was induced at two different stages of development (1st and 2nd instar larvae). However, this experiment indicates that cell death phenotype might be specific of the region where each actin-GFP is overexpressed, suggesting that the different cellular outcomes observed seem to be dependent on the region where cells are overexpressing each actin-GFP isoform.

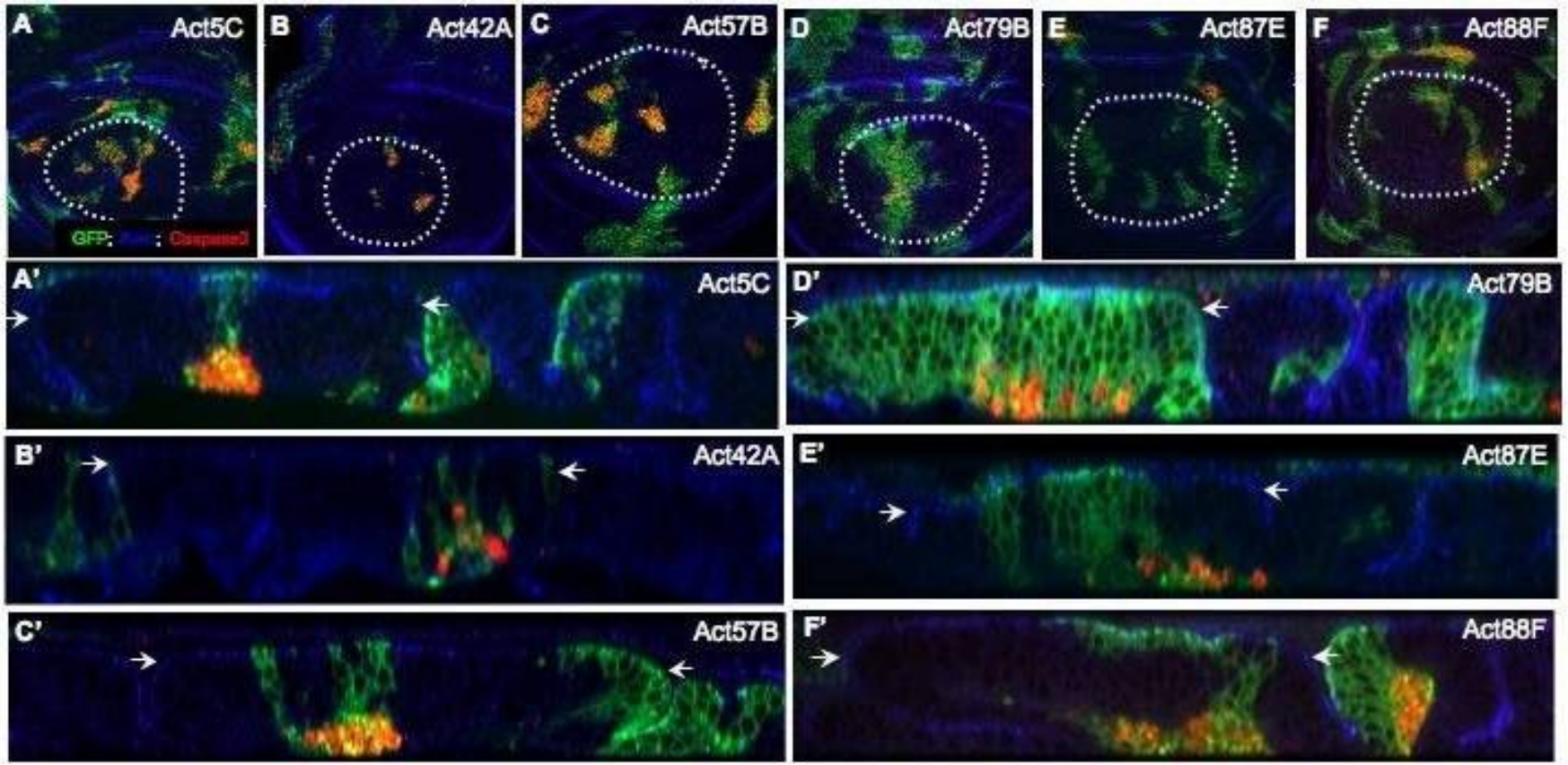

Fig. 4.9 – Groups of cells overexpressing actin genes give specific developmental phenotypes that are cell-type dependent. All panels show third instar wing imaginal discs in which overexpressing-clones are marked positively by GFP in green and stained with an anti-Armadillo antibody in blue to outline the apical cell membranes and an anti-activated-Caspase3 antibody in red, to stain Caspase-dependent cell death. (A-F) Standard confocal sections. The wing blade is delimited by a punctuated white line. (A'-F') Optical cross-sections through the wing disc epithelium. The white arrows in A'-F' define the wing blade region. Clones overexpressing the six *actin genes* lead to extrusion and death of cells mostly in the wing blade region.

4.4 – Some *actin 5C, 42A* and *57B*-overexpressing cells extrude from the wing blade epithelium and might survive.

Although clones of cells overexpressing *actin 5C, 42A* and *57B* extrude on the basal surface of the wing disc epithelium and die probably through a process of cell competition, many dying cells could also be recovered when these actin genes were overexpressed in the entire wing blade epithelium. To analyse if all the cells that extrude from the epithelium undergo apoptosis, I compared cross sections of discs overexpressing *actin 5C, 42A* and *57B* in the *nb*-expression domain and stained with an anti-Armadillo antibody (to outline the cell membrane) and an anti-activated Caspase 3 antibody (to show Caspase-dependant cell death) or with Phalloidin (to reveal F-actin) and with TOTO3 (to reveal the nuclei).

Many activated Caspase 3 or TOTO3 positive cells could be found on the basal surface of the wing blade epithelium, suggesting that *actin 5C, 42A and 57B* overexpressing cells have lost polarity and extrude from the epithelium (Fig. 4.10 A-C). Although cells contained activated-Caspase 3, suggesting that they were eliminated by apoptosis (Fig. 4.10 A-C), some might still be alive, since some TOTO3-positive cells were found on the basal surface of the wing blade epithelium (where no picnotic bright GFP staining was seen), which is an indication of dying cells (Fig. 4.10 A'-C'). However, some picnotic TOTO3-positive cells were found on the basal surface of the wing blade, suggesting that those cells might be dying (arrow in Fig. 4.10 B'). This phenotype could be clearly observed when *actin-42A-GFP* was overexpressed (Fig. 4.10 B') but weaker when either *actin-5C-GFP* or *57B-GFP* were overexpressed (Figure 4.10 A′, C′). The comparison between TOTO3 with picnotic TOTO3 staining, done in this experiment, suggests that, although the majority of cells that extrude from the wing blade epithelium die, some can still survive.

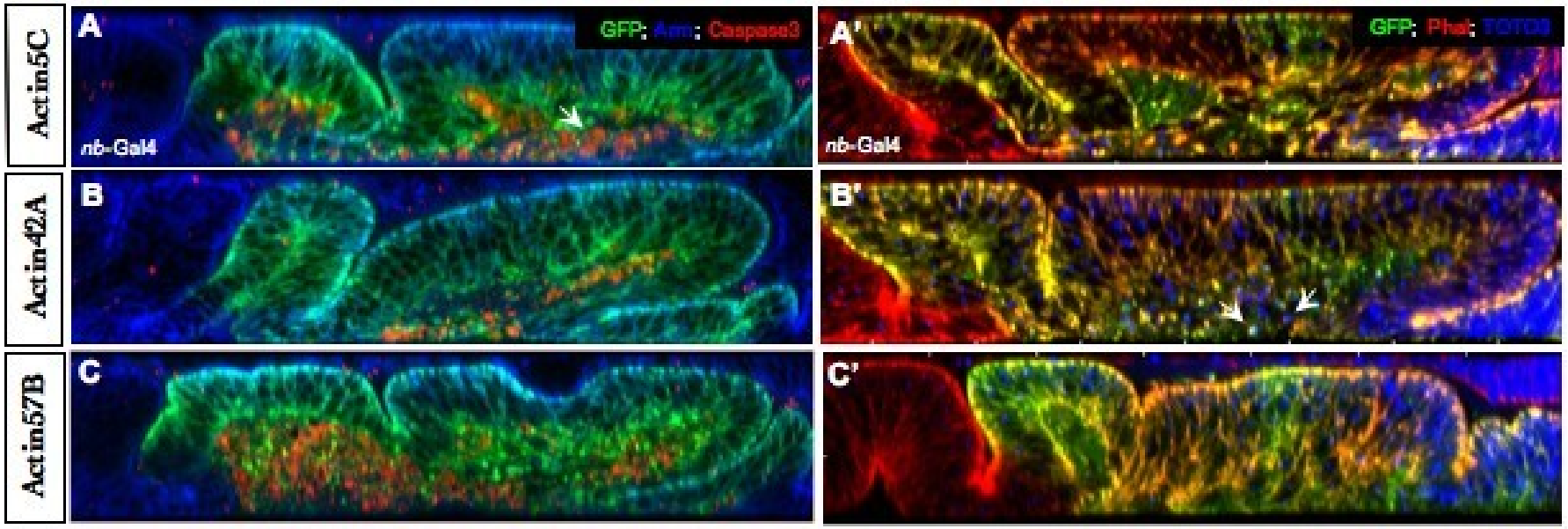

Fig. 4.10 – Overexpression of *actin 5C, 42A* and *57B* in the *nb*-expression domain leads to extrusion of cells that might survive. All panels show optical cross-sections through the wing disc epithelium of third instar wing imaginal discs. (A-C) Staining with GFP in green, which reveals each of the Actin-GFP fusion protein, Armadillo in blue, to outline the apical cell membrane, and activated-Caspase3 in red, which marks Caspase-dependant cell death. (A'-C') Staining with GFP in green, with Phalloidin in red, to mark F-actin, and TOTO3 in blue, to mark the nucleus of cells. The white arrow in A indicates Caspase-activated cells found on the basal surface of the wing blade. The white arrows in B' indicate TOTO3-positive cells and picnotic TOTO3-positive cells (brighter).

4.5 – Actin 5C, 42A, 57B, 87E and 88F overexpressing cells are recovered far away from where they were originated

Surprisingly, cells overexpressing either of the *actin-GFP* fusion, excluding actin 79B, could be recovered far away from where they were originated. When *actin 5C, 42A, 87E* and *88F* were overexpressed in the *en*-expression domain, GFP-positive cells originating from the posterior compartment were observed in the anterior compartment (Fig. 4.5 A''-C'' and E''-F''). In addition, *actin 57B*-overexpressing cells, induced in the *nb*-expression domain (Fig. 4.11 A') could be found in the proximal hinge region. I found that these cells contained activated Caspase 3, suggesting that these cells are not able to survive. The fact that some cells were recovered in a different region from where they originate suggests that these cells might have acquired the ability to migrate.

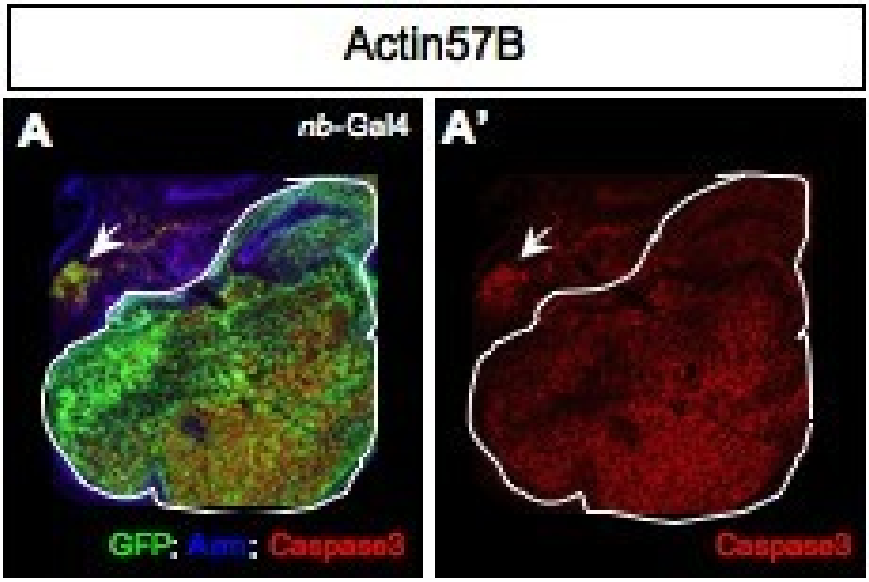

Fig. 4.11 – Overexpression of *actin 57B* in the *nb*-expression domain promote cell migration. The panels show standard confocal sections of third instar wing imaginal discs marked with GFP in green, which reveals each of the Actin-GFP fusion protein, and stained with an anti-Armadillo antibody in blue, to outline the apical cell membrane, and an anti-activated Caspase 3 in red, which mark Caspase-dependant cell death. (A) Merged. (A') Activated-Caspase 3 alone. The *nb*-expression domain is delimited with a white line.

V – Discussion

In this study I tried to address, by an overexpression approach, whether each *Drosophila* actin gene has specific functions during differentiation of the wing epithelium tissue. Either of the six actin genes were overexpressed using GFP tagged forms in wing imaginal discs using the UAS-Gal4 and the Gal80 systems. The developmental consequences of overexpressing each of the six actin genes during epithelial morphogenesis were analysed.

Each actin isoform might incorporate within specific actin filament structures.

To compare the consequences of the overexpression of each of the *actin-GFP* genes in disc epithelial tissues, it was essential to analyse their overexpression levels. While, all fly Actin-GFP fusion proteins display similar levels of overexpression, their overexpression in the wing imaginal discs give rise to distinct cellular defects and differential strength of such defects in the adult wings (see Results Fig. 4.1 and 4.3). The adult flies that overexpressed *actin 5C, 42A* or *57B* in the wing blade, displayed severely damaged and reduced wings, while flies overexpressing *actin 79B, 87E* or *88F* had less affected wings when the overexpression is carried out with the same driver (see Results Fig. 4.3). This indicates that the overexpression of *actin 5C, 42A* or *57B* is more deleterious for development of the wing proper than the overexpression of *actin 79B, 87E* or *88F*. These results were surprising since Roper and colleges (Roper *et al*., 2005) have observed that in most cases Actin-GFP overexpression did not interfere with cellular function when driven in various tissues, including the embryonic epidermis, the amnioserosa, the follicle epithelium or the larval muscles. In few exceptions, however, overexpression of Actin-GFP give rise to developmental consequences. For instance,

when driven in the indirect fly muscle, overexpression of either one Actin-GFP give a flightless phenotype of different strength. While only Actin 5C and 57B-GFP interfere with normal germline development. Although I cannot rule out the possibility that the divers Gal4 drivers I used to overexpressed each of the six actin gene in the wing imaginal disc are stronger, all together, my results suggest that differentiation of the wing imaginal disc require a tight regulation of the level of expression of each actin gene and more importantly of *actin 5C, 42A* and *57B*.

Not surprisingly, I found that, wing cells overexpressing either of the 6 actin-GFP isoforms promote excessive actin filaments formation highlighted by higher Phalloidin staining (see Results Fig. 4.2). This suggests that all actin fused to GFP are at least incorporated in actin filaments. However, the accumulation of actin filaments was found to be differential from one actin-GFP isoform to another (see Results Fig. 4.2). For instance, Actin 5C-GFP and 57B-GFP could promote excessive actin filaments at the basal surface of wing disc epithelium. In contrast, Actin 42A-GFP, 79B-GFP, 87E-GFP and 88F-GFP induced formation of excessive actin filaments at the apical surface of the wing disc epithelium. This indicates that each actin isoform incorporates in specific actin filament structures. For instance, Actin 5C and 57B might get incorporated in basal actin structures such as the stress fibers, while, Actin 42A, 79B, 87E and 88F might incorporate in more apical actin structures like the actin belt (Ursprung, 1972). Other actin-based structures have also been described in imaginal discs. Filopodia and lamellipodia have been shown to being located at basal and apical locations, respectively, in wing discs. Both these structures are involved in all motility and in cell-cell interaction. According to my data, Actin 5C and 57B are the isoforms that are preferentially observed basal, while 42A, 79B, 87E and 88F are mainly located apical. The hypothesis would be that the first isoforms would bundle into filopodia, while the second ones would do it to the lamellipodia. However, the level of my analysis was not accurate enough to verify this. Both these actin structures are very sensitive to the fixative protocols, therefore to verify these possibilities live imaging would be crucial.

In other epithelial model, such as the ovarium follicle epithelium, Röper and colleges (Röper *et al.*, 2005) have also found that, Actin 5C and 87E-GFP incorporate into filaments localized at similar cellular sites. However, the four other Actin-GFP

incorporate efficiently into actin structures localized at different locations. For instance, Actin 42A, 79B and 88F-GFP are incorporated more strongly into stress fibers than into cortical actin Together, the comparison between these two epithelial tissues, wing imaginal discs and the ovarium follicle, suggests that the incorporation of the different actin isoforms into the actin structures is specific of each epithelium.

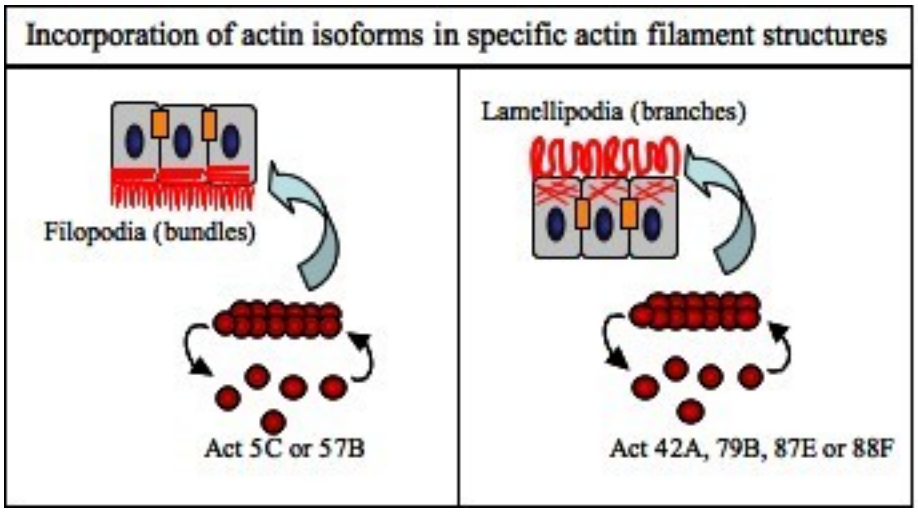

Figure 5.1 – Model for specific incorporation of the six actin isoforms into filopodia structures (formed of actin filaments bundles) or into lamellipodia structures (formed of actin filaments branches).

How could the primary actin protein sequence lead to the preferable incorporation of one actin over another for a single filament within an actin structure? One possibility is that ABPs that support the formation of certain structures could show a preference for certain actins. An example of such preference has been described in the protein beta cap73 that preferentially binds to β-actin but not α-actin (Shuster *et al*., 1996). Such preferential binding of accessory proteins could explain the striking difference of incorporation into branch or bundles at different location within the cell. This suggest that the specific interaction between each actin isoform actin and ABPs may control where and when specific actin monomer would be incorporated into actin filaments, in addition to the type of filaments network they should form.

Epithelia are not equivalent in terms of actin cytoskeleton organization.

The overexpression of either of the six actin isoforms in the wing imaginal disc lead to specific developmental phenotypes. The different cellular behaviours observed seem to be region specific and time specific (see Results Fig. 4.7 and 4.9).

My clonal analysis revealed that in the blade and hinge region of the disc, cells overexpressing each of the *actin-GFP* genes seems to have lost their polarity and were found on the basal surface of the wing disc, where they are likely to be eliminated by apoptosis since they expressed activated Caspase-3 (see Results Fig. 4.9). In contrast to the notum, fewer *actin-GFP* overexpressing cells showed this behaviour (see Results Fig. 4.9). This suggests that the wing blade and hinge epithelia are more sensitive to *actin-GFP* overexpression and possess distinct properties from the notum epithelia.

Using *sd*-Gal4 or *en*-Gal4 driver, which expresses the target genes at early stages of larval development, the overexpression of *actin 5C-GFP* and *57B-GFP* promote a reduced wing blade (see Results Fig. 4.7). However, these effects were not observed using the *nb*-Gal4 driver (see Results Fig. 4.7), which expresses the target gene at later stages. This indicates that the overexpression of *actin 5C* and *57B* might prevent growth of the wing blade only at early larval stages, while has no effect on cell growth at later stages, suggesting a time-dependent effect.

The fact that, the different cellular behaviours observed seems to be region and time specific, suggest that epithelia of different regions of the wing disc, but also during different developmental stages, are not equivalent in term of cytoskeletal organization and/or junctional properties. Indeed, wing blade epithelial cells extend cytonemes oriented towards the AP and/or DV boundary, while, hinge epithelial cells do not extend cytonemes and notum cells radiate short cytonemes in all directions (Hsiung *et al*., 2005). Also, differences in cell shape could be observed between different regions of the wing imaginal disc: At early third instar, while the hinge and notum epithelia maintain their

cuboidal shape, blade epithelial cells acquire a columnar shape (Shen and Dahmann, 2005). Furthermore, a Microarray analysis showed that the *actin 57B* mRNA is strongly expressed in the notum region (Butler *et al.*, 2003), suggesting that Actin 57B might be required to pattern the notum of the animal. Alternatively, downregulation of actin 57B may be important for the wing blade to be form. However, we don't know which actin gene is expressed in the wing imaginal disc and whether they are transcriptionally regulated over time or in different wing regions.

RNA blot hybridization experiments showed that *actin 5C* and *42A* are both expressed during larval stages (Fyrberg *et al*., 1983). Since both are cytosplasmic actins, they should be expressed in all discs epithelia, including the wing epithelial tissue. Among the four muscle-specific genes, *actin 57B* is mostly expressed in embryonic and larvae muscles (Fyrberg *et al*., 1983), suggesting that wing discs epithelial tissues may not contain this isoforms. Although Actin 87E is expressed throughout life, no published data argue that this actin isoform takes part during differentiation of the disc epithelia. In addition, since actins 79B and 88F are expressed mostly in pupae and adults (Fyrberg *et al.*, 1983), they are unlikely to have a major role during wing imaginal disc development. However, recent studies indicate that low levels of other actins are present in various tissues (Nongthomba *et al*., 2001). This suggests that in my experiments, while I overexpressed actin 5C, 42A and 57B in the whole wing disc or in the notum, I misexpressed actin 57B or 87E, 79B and 88F where normally they are not. In order to analyse which actin gene is expressed in the wing imaginal disc and whether their expression pattern vary along the proximo-distal axis of the wing imaginal disc, I performed *in situ* hybridization experiments on third instar wing tissues, using specific anti-sense probes directed against the 3'UTR of each actin gene. I compared the signal given by the anti-sense probe for each actin to the one of a sense probe used as a negative control. Preliminary data showed that *actin 5C, 42A* and *57B* mRNA are expressed in wing imaginal discs (see Appendix II). Each of them may not be transcribed at the same level in the whole wing imaginal disc. For instance, Actin 5C mRNA seems to be expressed mainly in the wing blade region (see Appendix II). This would suggest that the upregulation of this actin isoform is required for the proper formation of the blade region of the wing disc or that downregulation of Actin 5C promotes development of the notum

and hinge regions of the disc. These experiments require to be confirmed since the results were not always consistent from one disc to another. However, if in future experiments I observe that actin genes are transcriptionally regulated in specific region of the wing disc, this would strongly argue that organization of the actin cytoskeleton is specific in each region of the wing disc epithelium.

Actin 5C, 42A and 57B might affect Hippo signalling.

Overexpression of *actin 5C-GFP*, *42A-GFP* and *57B-GFP* by using Gal4 drivers expressed in the hinge (including *en*-Gal4, *nb*-Gal4 or *sd*-Gal4), resulted in wing hinge expansion (see Results Fig. 4.5 and see Appendix I), associated to Wg upregulation (see Results Fig. 4.6). However, overexpression of *actin 79B-GFP*, *87E-GFP* and *88F-GFP* in the same expression domains did not induce such effects. Assuming, as discussed before, that I overexpressed each actin genes at similar levels, these two groups of actin isoforms behave differently when overexpressed in the hinge. This indicates that endogenous expression of *actin 5C, 42A* and *57B* has to be tightly regulated to restrict hinge growth.

Interestingly, depletion of either subunit of the Capping Protein heterodimer (CP), which induces excessive actin polymerization, gives a similar phenotype: promotes hinge overgrowth associated to Wg upregulation (Janody, unpublished). In addition, loss of CP induces upregulation of *expanded* (*ex*) in the hinge region. Both *wg* and *ex* are well-known target genes of the Hippo pathway, which is required to restrict cell and tissue growth in *Drosophila.* Activation of the Hippo (Hpo)/Salvador (Sav) kinase complex, via the two ERM protein Expended (Ex)/ Merlin (Mer), in turn activates the Warts/Mats kinase complex. Warts/Mats kinase phosphorylates and inhibits Yorkie (Yki), a transcription coactivator that positively regulates cell growth, survival and proliferation (Fig. 5.2). Indeed, mutations for components of this pathway exhibit dramatic outgrowths in a variety of fly epithelial tissues and were shown implicated in human cancer (Saucedo and Edgar, 2007). Therefore, my results suggests that capping of Actin 42A, 5C, 57B by

CP regulate Hpo signaling directly. Although, the Hpo pathways have been extensively analyzed, the exact source of the input signals, though regulation of the NF2 tumor suppressor Mer and Ex, is still largely unknown. ERM family proteins, such as Mer, form a structural linkage between transmembrane components and the actin cytoskeleton and Mer has been reported to bind numerous cytoskeletal factors (Edgar *et al*., 2006). Loss of *CP* or overexpression of *actin 42A, 5C* or *57B* might compromise the plasma membrane-cytoskeletal cross-linking required to promote the growth inhibitor function of Hippo required to prevent cell growth (Fig. 5.2). A possible way to test this hypothesis, is by analysing whether Yorkie target genes, such as *ex* and *mer* themselves (or *diap1* and *cyclin E*) are up-regulated in situations where Actin 5C, 42A and 57B are overexpressed. In addition, a genetic interaction between each actin gene that gives this overgrowth phenotype and the target genes of the Hippo pathway, mentioned before, should also be analysed.

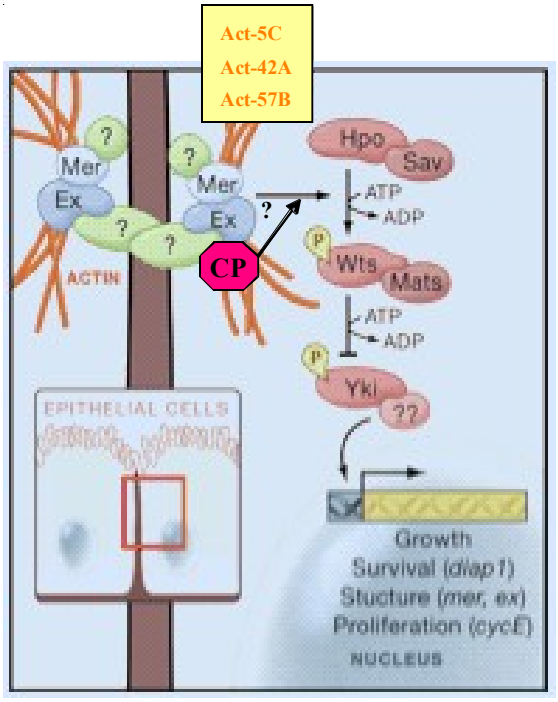

Figure 5.2 – Schematic representation of the model of Hippo pathway to explain the hinge overgrowth phenotype associated to Wg upregulation observed when the *cp* is depleted or the *actin 5C, 42A* or *57B* are overexpressed (adapted from Edgar, 2006).

Apart from hinge overgrowth, I also observed in the wing hinge region a large number of cell deaths associated to *actin 5C*, *42A* and *57B* overexpression. This suggests that although the majority of cells lose their proliferation control and overproliferate, some are not able to survive and undergo apoptosis. This contradictory phenotype observed, might be a consequence of two different mechanisms occurring at the same time in that region of the disc. Such possibility should be further studied.

CP might prevent polymerization of Actin 42A to maintain cells within the wing blade epithelium.

Interestingly, very few cells overexpressing *actin 42A* could be recovered in the posterior compartment of the wing blade when driven with the *en*-Gal4 driver (see Results Fig. 4.8). Also, groups of cells overexpressing *actin 42A*, surrounded by wild type cells (in a clonal situation), extrude from the epithelium and seem to die by apoptosis (see Results Fig. 4.9 B). However, targeting overexpression of *actin 42A* in the whole wing blade (by using the *sd*-Gal4 driver) induces a clear expansion of the wing blade (see Results Fig. 4.8), suggesting that these cells proliferate. Overexpression of the other actin genes did not show such different outcomes depending of the cellular context. This indicates that a type of short-range-interaction between cells expressing different levels of Actin 42A, called cell competition mechanism, is occurring (reviewed in Moreno, 2008). All together, these suggest that *actin 42A*-overexpressing cells, when apposed to wild type cells, are eliminated by a process of cell competition.

Cell competition was also observed when *cpb* is depleted. In a clonal situation, *cpb* mutant cells extrude basally and die (Janody and Treisman, 2006), while broad depletion of *cpb* by RNA interference in the *sd*-Gal4 expression domain leads to tissue overgrowth (Janody, unpublished data). In addition, similar to *cpb* depletion, when *actin 42A* was overexpressed in the entire wing blade epithelium, some activated Caspase 3

positive cells were found on the basal surface of the wing blade epithelium, suggesting that *actin 42A* overexpressing cells may have lost polarity, extruded from the epithelium and died by apoptosis (see Results Fig. 4.10 B). Interestingly, some TOTO3 positive cells that do not seemed pycnotic were not marked with the anti-Caspase 3 antibody, indicating that some cells might still survive (see Results Fig. 4.10 B').

This behaviour recapitulates many aspect of cells in which the activity of the Src protoncogene is enhanced in the wing imaginal disc (Langton *et al*., 2007; Vidal *et al*., 2006). Furthermore, like Src (Yeatman, 2004), CP colocalized with components of adherens junction, prevented the mislocalization of adherens junction components and the activation of JNK signaling (Janody and Treisman, 2006).

Since the Src substrate is activated for phosphorylation by mechanical unfolding (Vogel *et al*., 2006), this suggests that uncapping Actin 42A by CP promotes an increased in intracellular mechanical forces that induces Src activation. Src activation then, will lead to activation of the JNK pathway, which is the ultimate responsible for either inducing cell death or proliferation. All together, these evidences might suggest that CP might prevent specifically the polymerization of Actin 42A to restrict the Src activity at the AJ.

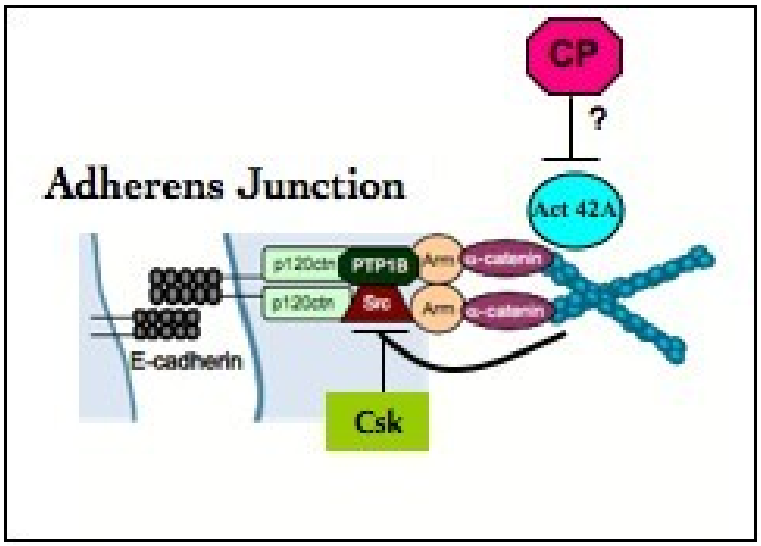

Figure 5.3 – Schematic representation of the model of SRC hypothesis to explain the cell death phenotype in the blade, observed when the *cp* is depleted or when *actin 42A* is overexpressed in clones of cells (adapted from Yeatman, 2004).

All actin isoforms, excluding Actin 79B, might provide to epithelial cells the ability to migrate.

Surprisingly, cells overexpressing either of the *actin-GFP* fusion, excluding actin 79B, could be recovered far away from where they were originated (see Results Fig. 4.5 and 4.11), suggesting that these cells may have acquired the ability to migrate. However, these cells might not be able to survive since they expressed activated Caspase 3.

Interestingly, cells in movement accumulate more actin filaments when compared to static cells. Cell migration is coordinated by a highly dynamics meshwork of actin filaments. At the leading edge, this actin network is used to move the cell by prolonging and crosslinking existing filaments and thereby pushing the cell membrane forward (Zimmermann, 2001). In my experiments, overexpression of each actin isoform lead to an excessive accumulation of actin filaments in epithelial cells, suggesting that promoting accumulation of actin filaments increases the rate of polymerization and faster actin treadmilling that lead to increase cell mobility. However, overexpression of *actin 79B* did not lead to GFP-positive cell found far away from where they originate. Although it remains possible that these cells could not be observed if they had already died, it suggests that the subpopulation of actin filament promoted by Actin 79B overexpression does not promote cell mobility. Interestingly, Roper and colleges (Roper *et al*., 2005) also found a striking difference in cellular behaviour between cells overexpressing actin 79B-GFP to cells overexpressing the other actin genes.

VI – References

VII – Appendix

Appendix I

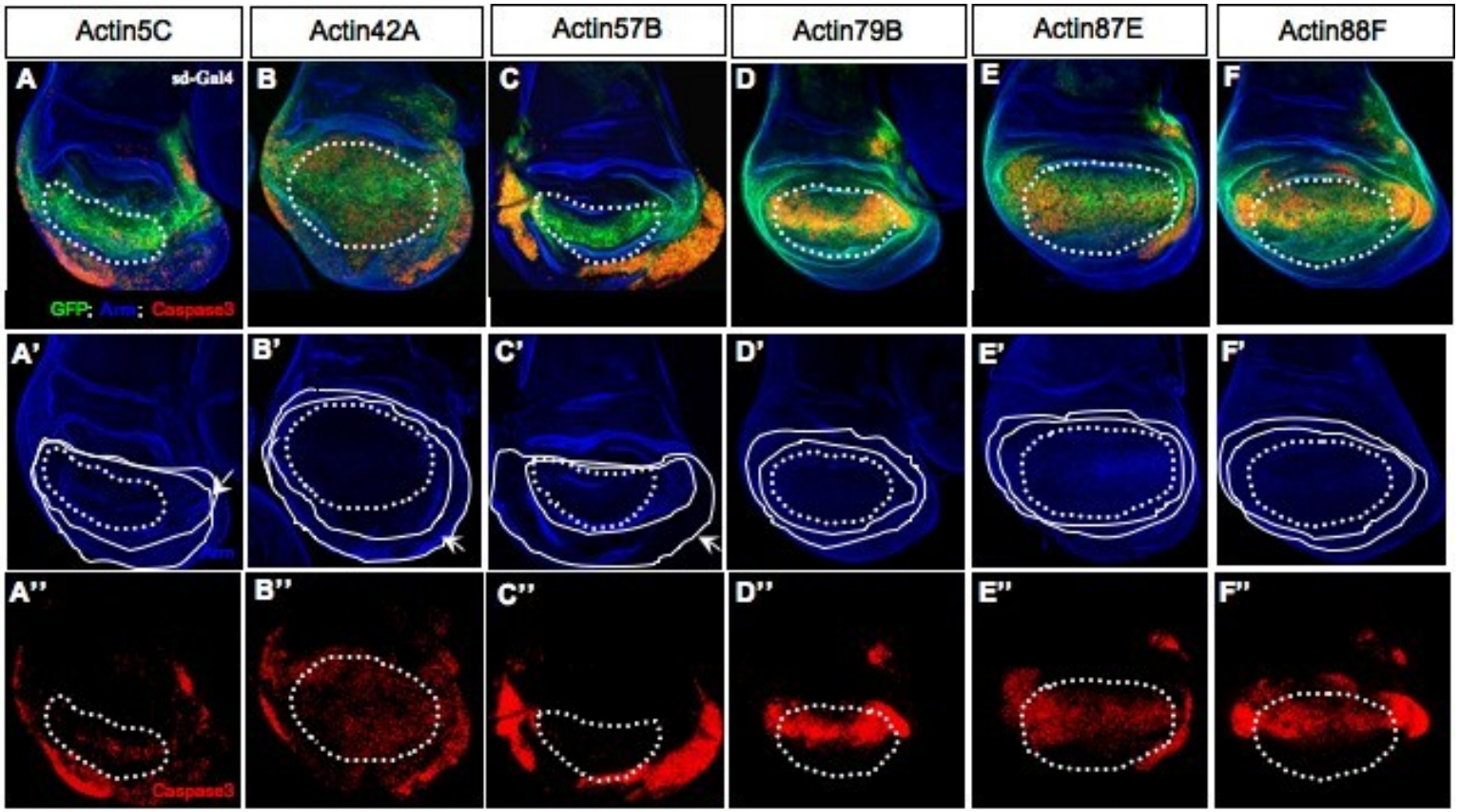

Figure I.1 – Overexpression of Actin 5C-GFP, 42A-GFP and 57B-GFP, with *sd*-Gal4 driver, promote hinge expansion. All panels show standard confocal sections of third instar wing imaginal discs marked with GFP in green, which reveals each of the Actin-GFP fusion protein, Armadillo in blue, which outline the apical cell membrane and activated-Caspase3 in red, which mark Caspase-dependant cell death. (A-F) Merged. (A'-F') Armadillo alone, with wing blade and hinge delimited. (A''-F'') Activated-Caspase3 alone with wing blade delimited. The white arrows in A', B' and C' indicate hinge overgrowth. (A''-F'') Overexpression of all actin genes leads to death in wing hinge and blade, except for actin 57B that does not lead to death in the wing blade.

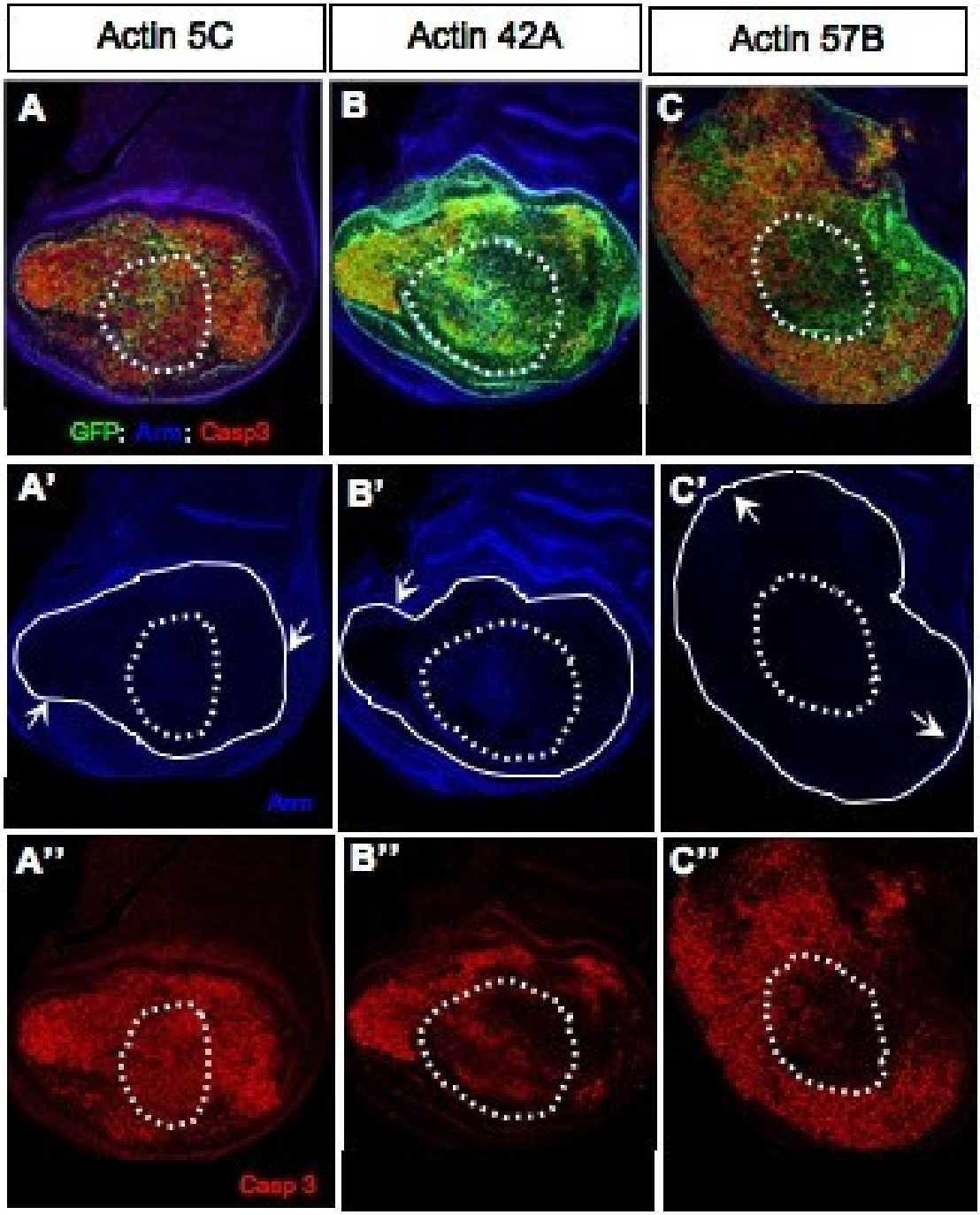

Figure I.2 – Overexpression of Actin 5C-GFP, 42A-GFP and 57B-GFP, with *nb*-Gal4 driver, promote hinge expansion. All panels show standard confocal sections of third instar wing imaginal discs marked with GFP in green, which reveals each of the Actin-GFP fusion protein, Armadillo in blue, which outline the apical cell membrane and activated-Caspase3 in red, which mark Caspase-dependant cell death. (A-C) Merged. (A'-C') Armadillo alone with wing blade and hinge delimited. (A''-C'') Activated-Caspase 3 alone with wing blade delimited. The white arrows in A', B' and C' indicate hinge overgrowth. (A''-C'') Overexpression of actin 5C-GFP, 42A-GFP and 57B-GFP leads to death in the wing hinge and blade.

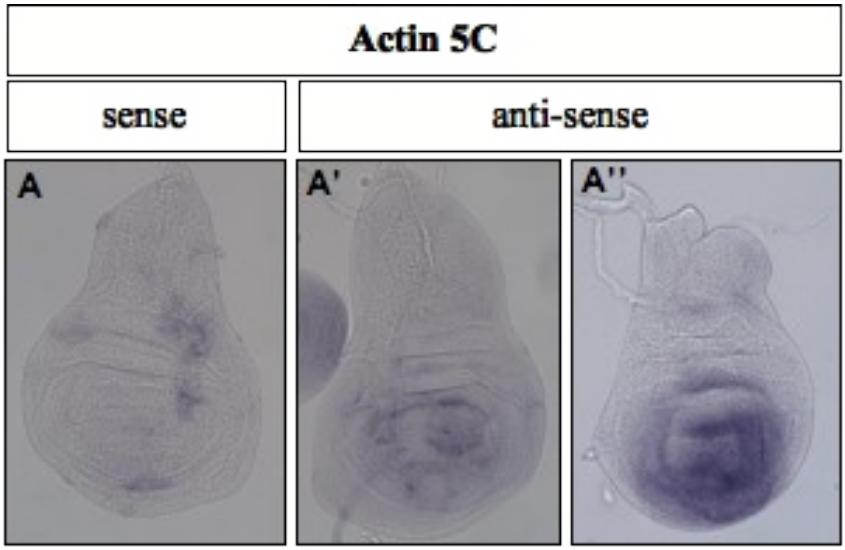

Figure II.1 – Expression of Actin 5C mRNA in wing imaginal discs. (A) *In situ* hybridization using a sense *actin 5C*-3'UTR probe, giving no signal, demonstrating the specificity of the antisense probe. (A'-A'') *In situ* hybridization using an antisense *actin 5C*-3'UTR probe.

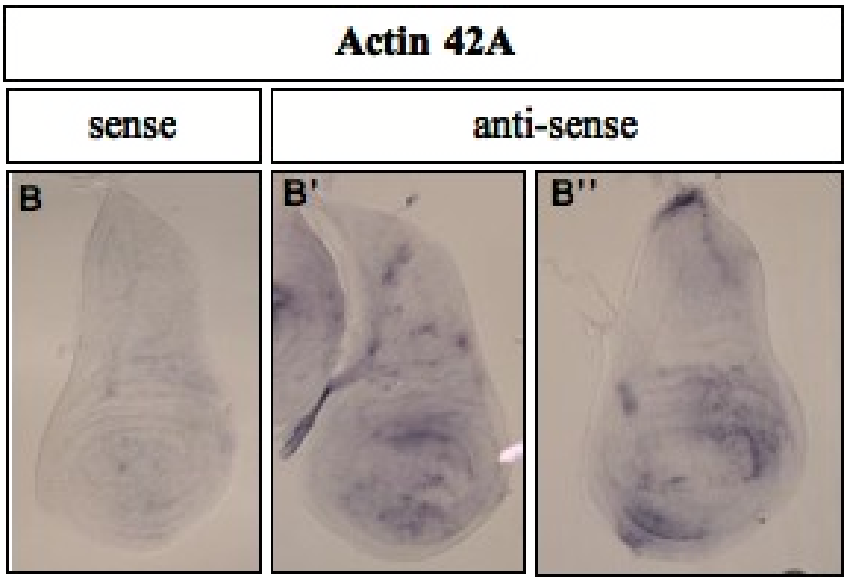

Figure II.2 – Expression of Actin 42A mRNA in wing imaginal discs. (B) *In situ* hybridization using a sense *actin 42A*-3'UTR probe, giving no signal, demonstrating the specificity of the antisense probe. (B'-B'') *In situ* hybridization using an antisense *actin 42A*-3'UTR probe.

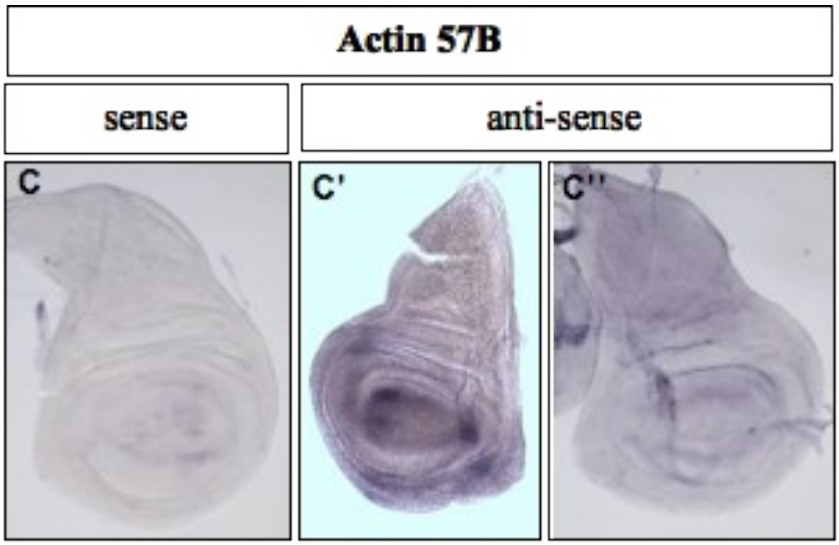

Figure II.3 – Expression of Actin 57B mRNA in wing imaginal discs. (C) *In situ* hybridization using a sense *actin 57B*-3'UTR probe, giving no signal, demonstrating the specificity of the antisense probe. (C'-C'') *In situ* hybridization using an antisense *actin 57B*-3'UTR probe.